5

WALL-BOUNDED SHEAR FLOWS

Boundary-layer flows are more complicated than flows in free shear layers because the presence of a solid wall imposes constraints that are absent in wakes and jets. The most obvious constraint is that the viscosity of the fluid, no matter how small it is, enforces the no-slip condition: the velocity of the fluid at a solid surface must be equal to the velocity of the surface. This viscous constraint gives rise to a viscosity-dominated characteristic length, which is of order ν/w if w is characteristic of the level of turbulent velocity fluctuations. At large Reynolds numbers, the boundary-layer thickness δ is much larger than ν/w, so that we have to deal with two different length scales simultaneously. This problem will be thoroughly discussed for turbulent flow in channels and pipes. After the consequences of the presence of more than one length scale are fully understood, turbulent boundary layers in the atmosphere and turbulent boundary layers in pressure gradients will be studied.

5.1
The problem of multiple scales

It is instructive to take a preliminary look at the problem of multiple scales. We do so in a qualitative way, leaving the analytical details for Section 5.2. The solid wall may be smooth or rough, so that we have a small viscous length ν/w or a characteristic height k of the roughness elements in addition to the boundary-layer thickness δ. Because δ is generally much larger than ν/w and/or k, we expect that the latter do not influence the entire flow. Instead, we expect that these small length scales control the dynamics of the flow only in some narrow region in the immediate vicinity of the surface. This region, called the wall layer or surface layer, has an asymptotic behavior in the limit as $\delta w/\nu \to \infty$ or $\delta/k \to \infty$, which is quite distinct from the overall development of the boundary layer. Therefore, we must treat boundary layers in a piecemeal fashion by first dealing with the surface layer and the rest of the flow (which is called the outer layer) separately and then reconciling these partial descriptions with appropriate asymptotic methods.

As in boundary-free shear flows, a comprehensive analysis of boundary-layer flows can be performed only if the downstream evolution is slow. If L is a streamwise length scale, we need to require that $\delta/L \ll 1$ in order to make sure that only the local scales δ, ν/w, and w are relevant in the dimensional analysis.

Inertial sublayer There exists a close analogy between the spatial structure of turbulent boundary layers and the spectral structure of turbulence. At sufficiently large Reynolds numbers, the overall dynamics of turbulent boundary layers is independent of viscosity, just as the large-scale spectral dynamics of turbulence is. In the wall layer of a turbulent boundary layer, viscosity generates a "sink" for momentum, much like the dissipative sink for kinetic energy at the small-scale end of the turbulence spectrum. In particular, the asymptotic rules governing the link between the large-scale description and the small-scale description lead to the closely related concepts of an inertial subrange in the turbulence energy spectrum (see Chapter 8) and an inertial sublayer in wall-bounded shear flows. In the literature, the inertial sublayer is called the logarithmic region because its mean-velocity profile is logarithmic, as we shall see later.

A preview of the concept of an inertial sublayer is in order. If the length-scale ratio $\delta w/\nu$ is large enough, it should be possible to find a range of distances y from the surface such that $yw/\nu \gg 1$ and $y/\delta \ll 1$ simultaneously. In this region, the length scale ν/w is presumably too small to control the dynamics of the flow, and the length scale δ is presumably too large to be effective. If this occurs, the distance y itself is the only relevant length.

A graphical representation of the situation is given in Figure 5.1. If w is representative of the turbulence intensity and if no other characteristic velocities occur in the problem, the mean-velocity gradient $\partial U/\partial y$ can depend on w and y only in the following way:

$$\partial U/\partial y = cw/y. \tag{5.1.1}$$

This integrates to

$$U/w = c \ln y + d. \tag{5.1.2}$$

Under the assumptions already stated, (5.1.1) is a dimensional necessity, so that we may expect to find a logarithmic velocity profile wherever $yw/\nu \gg 1$ and $y/\delta \ll 1$ (see also Section 2.5).

In most boundary-layer flows, the velocity scale w is not known a priori. It turns out that (5.1.2) is a crucial link in the determination of the dependence of w on the independent variables of the problem.

Velocity-defect law As in wake flow, the scaling length for most of the boundary layer (with exclusion of the surface layer) is the thickness δ. This is

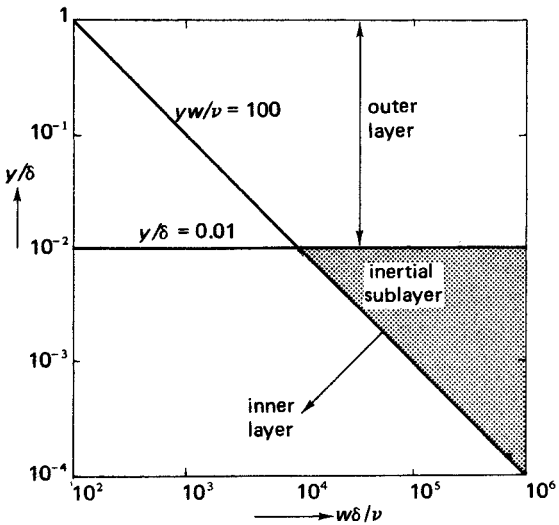

Figure 5.1. An inertial sublayer can exist only if the Reynolds number is large enough. For illustrative purposes, $yw/\nu >> 1$ and $y/\delta << 1$ have been interpreted as $yw/\nu > 100$, $y/\delta < 0.01$. For many practical applications, the limits do not need to be as strict as this.

the appropriate length because the large eddies in the flow have sizes comparable to δ. If the turbulence in a boundary layer is driven by Reynolds stresses, the mean-velocity gradient $\partial U/\partial y$, which is the reciprocal of a "transverse" time scale for the mean flow, has to be of order w/δ if w is the scaling velocity for the Reynolds stress. This argument does not apply to the flow near the surface, because the length scale is different there. The differential similarity law

$$\partial U/\partial y = (w/\delta)\, f(y/\delta) \tag{5.1.3}$$

thus has to be integrated from outside the boundary layer toward the wall in order to obtain a similarity law for U. The result is

$$U - U_0 = -(w/\delta) \int_y^\infty f(y/\delta)\, dy = wF(y/\delta), \tag{5.1.4}$$

where U_0 is the velocity outside the boundary layer. We find later in this chapter that self-preservation can be obtained only if $w/U_0 << 1$. However, a velocity defect $(U_0 - U)$ of order w can never meet the no-slip condition $U_0 - U = U_0$ at the surface if $w/U_0 << 1$. This indicates that a dynamically

distinct surface layer with very steep velocity gradients must exist in order to satisfy the boundary condition. If the velocity and length scales in the surface layer are w and ν/w, respectively, the velocity gradients must be of order w^2/ν; hence, they are very large compared to the velocity gradients in the outer layer (which are of order w/δ) if $w\delta/\nu$ is large enough.

5.2
Turbulent flows in pipes and channels

The equations of motion for turbulent flows in pipes and in channels with parallel walls are relatively simple, because the geometry prohibits the continuing growth of their thickness. If the pipe or channel is long enough, the velocity profile has to become independent of the downstream distance x. As a result, the nonlinear inertia terms $U_j\partial U_i/\partial x_j$ are suppressed. This simplifies the theoretical analysis considerably and separates the surface layer–outer layer problem from the problems associated with the downstream development in other wall-bounded shear flows.

Channel flow We consider turbulent flow of an incompressible fluid between two parallel plates separated at a distance $2h$. The plates are assumed infinitely long and wide; they are at rest with respect to the coordinate system used. A definition sketch is given in Figure 5.2. The mean flow is assumed to be in the x,y plane and steady, and all derivatives of mean quantities normal to that plane are assumed to be zero. All derivatives with respect to x are also assumed to be zero, except for the pressure gradient dP/dx, which drives the

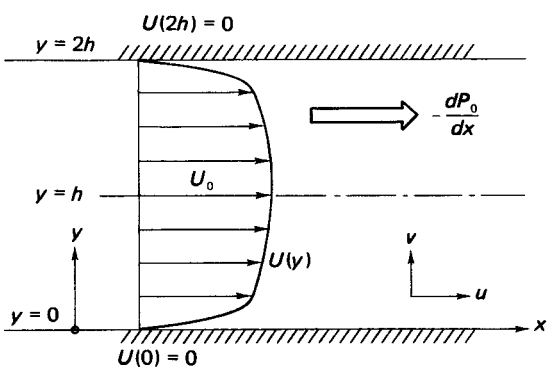

Figure 5.2. Definition sketch for flow between plane parallel walls.

flow against the shear stresses at the two walls. The continuity equation requires that the y component of the mean velocity is zero everywhere if it is zero at both walls.

The relevant equations of motion for the mean flow are

$$0 = -\frac{1}{\rho}\frac{\partial P}{\partial x} - \frac{d}{dy}\overline{uv} + \nu\frac{d^2U}{dy^2}, \tag{5.2.1}$$

$$0 = -\frac{1}{\rho}\frac{\partial P}{\partial y} - \frac{d}{dy}\overline{v^2}. \tag{5.2.2}$$

Integration of (5.2.2) yields

$$P/\rho + \overline{v^2} = P_0/\rho, \tag{5.2.3}$$

where P_0 is a function of x only. Because $\overline{v^2}$ is independent of x (by assumption), $\partial P/\partial x$ is equal to dP_0/dx. Both of these gradients should be independent of x to avoid streamwise acceleration of the flow. Therefore, (5.2.1) can be integrated from $y = 0$ upward, to yield

$$0 = -\frac{y}{\rho}\frac{dP_0}{dx} - \overline{uv} + \nu\frac{dU}{dy} - u_*^2. \tag{5.2.4}$$

As in Section 2.5, the stress at the surface has been defined as ρu_*^2; the velocity u_* is called the *friction velocity*. The turbulent velocity fluctuations have to satisfy the no-slip condition, so that the Reynolds stress is zero at the surface. The surface stress is thus purely viscous stress.

At the center of the channel ($y = h$), the shear stress ($-\rho\overline{uv} + \mu\, dU/dy$) must be zero for reasons of symmetry. Hence, if $y = h$, (5.2.4) reads

$$u_*^2 = -\frac{h}{\rho}\frac{dP_0}{dx}. \tag{5.2.5}$$

In this problem the shear stress at the wall is determined by the pressure gradient and the width of the channel only, which is one reason why this flow is less complicated than others.

If we use (5.2.5) to substitute for dP_0/dx in (5.2.4), we obtain

$$-\overline{uv} + \nu\frac{dU}{dy} = u_*^2\left(1 - \frac{y}{h}\right). \tag{5.2.6}$$

Contemplating possible nondimensional forms of (5.2.6), we conclude that u_*^2 is the proper scaling factor for $-\overline{uv}$ because we expect the viscous stress

to be small at large Reynolds numbers. Also, the experience gained in the study of wakes suggests that $\partial U/\partial y$ should be scaled with u_*/h, because the turbulent scales of velocity and length presumably are u_* and h. Thus, we should write

$$-\frac{\overline{uv}}{u_*^2}+\frac{\nu}{u_* h}\frac{d(U/u_*)}{d(y/h)}=1-\frac{y}{h}. \tag{5.2.7}$$

If the Reynolds number $R_*=u_*h/\nu$ is large, this particular nondimensional form suppresses the viscous stress. Because the stress at the surface is purely viscous, (5.2.7) cannot be valid near the wall in the limit as $R_*\to\infty$. In the immediate vicinity of the wall, therefore, another nondimensional form of (5.2.6) must be found; it should be selected in such a way that the viscous term does not become small at large Reynolds numbers. From (5.2.7) we conclude that this can be done by absorbing R_* in the scale for y. The resulting equation is

$$-\frac{\overline{uv}}{u_*^2}+\frac{d(U/u_*)}{d(yu_*/\nu)}=1-\frac{\nu}{hu_*}\frac{yu_*}{\nu}. \tag{5.2.8}$$

It is clear that this nondimensionalization tends to suppress the change of stress in the y direction if $R_*=u_*h/\nu\to\infty$.

For convenience, let us define

$$y_+\equiv yu_*/\nu, \quad \eta\equiv y/h. \tag{5.2.9}$$

Equations (5.2.7) and (5.2.8) then can be written as

$$-\frac{\overline{uv}}{u_*^2}+R_*^{-1}\frac{d}{d\eta}\left(\frac{U}{u_*}\right)=1-\eta, \tag{5.2.10}$$

$$-\frac{\overline{uv}}{u_*^2}+\frac{d}{dy_+}\left(\frac{U}{u_*}\right)=1-R_*^{-1}y_+. \tag{5.2.11}$$

We are looking for asymptotic solutions of these equations in the limit as $R_*\to\infty$. From (5.2.10, 5.2.11) it is evident that these solutions depend on our point of view: for all but very small values of η we expect the viscous stress to be negligibly small, and at finite values of y_+ (which correspond to very small values of η) we expect that viscous stresses are important and that the total stress is approximately constant. The region of viscous effects must

be confined to the immediate vicinity of the wall, since only there can we expect the local Reynolds numbers Uy/ν and y_+ to be so small that turbulence cannot sustain itself.

In the limit as $R_* \to \infty$, but with η remaining of order one, (5.2.10) reduces to

$$-\overline{uv}/u_*^2 = 1 - \eta. \tag{5.2.12}$$

This equation cannot represent conditions as $\eta \to 0$, which corresponds to finite values of y_+. We call the part of the flow governed by (5.2.12) the *core region* (the name "outer layer" is not appropriate in channel flow).

In the limit as $R_* \to \infty$, but with y_+ remaining of order one, (5.2.11) becomes

$$-\frac{\overline{uv}}{u_*^2} + \frac{d(U/u_*)}{d(yu_*/\nu)} = 1. \tag{5.2.13}$$

This equation cannot represent reality if $y_+ \to \infty$, which corresponds to finite values of η. The part of the flow governed by (5.2.13) is called the *surface layer*.

The surface layer on a smooth wall We now restrict ourselves momentarily to flow over smooth surfaces, so that the roughness height k does not occur as an additional parameter. The flow in the surface layer is governed by (5.2.13), which is free of explicit dependence on parameters. If the surface is smooth, no additional parameters occur in the boundary conditions on (5.2.13), so that we may expect the solution of (5.2.13) to be

$$U/u_* = f(y_+), \tag{5.2.14}$$

$$-\overline{uv}/u_*^2 = g(y_+). \tag{5.2.15}$$

These relations are called the *law of the wall*. The only boundary conditions that the system (5.2.13, 5.2.14, 5.2.15) needs to satisfy at this point are $f(0) = 0, g(0) = 0$. The similarity expressions (5.2.14, 5.2.15) may not be valid if $y_+ \to \infty$, unless that limit is approached rather carefully. The shapes of f and g have been determined experimentally, but we prefer not to discuss the experimental evidence before we have taken a look at the other side of the coin.

The core region In the core region, all we have is a statement, (5.2.12), on the Reynolds stress. The momentum equation thus gives no explicit information on U itself. Let us look at an equation in which U does occur explicitly. Such an equation is the turbulent energy budget, which in this channel-flow geometry is

$$-\overline{uv}\frac{dU}{dy} = \epsilon + \frac{d}{dy}\left(\frac{1}{\rho}\overline{vp} + \tfrac{1}{2}\overline{q^2 v}\right). \tag{5.2.16}$$

In (5.2.16), ϵ stands for the viscous dissipation of the turbulent kinetic energy $\frac{1}{2}\overline{q^2}$; viscous transport of $\frac{1}{2}\overline{q^2}$ has been neglected (see Chapter 3). Referring back to (5.2.12), we see that the Reynolds stress $-\overline{uv}$ is of order u_*^2 for all finite values of η. Since the turbulent energy is generated by this stress, we expect q^2 and p/ρ to be of order u_*^2, too. We have seen before that the large eddies in turbulent flows scale with the cross-stream dimensions for the flow. Hence, the terms on the right-hand side of (5.2.16) must be of order u_*^3/h. Since the Reynolds stress is of order u_*^2, we conclude that dU/dy is of order u_*/h. If we stay well above the surface layer, so that no other characteristic lengths can complicate the picture, we can state without any loss of generality that

$$\frac{dU}{dy} = \frac{u_*}{h} \cdot \frac{dF}{d\eta}, \tag{5.2.17}$$

with the understanding that $dF/d\eta$, which is the derivative of some unknown function F, is of order one. Because h is not an appropriate length scale near the surface, (5.2.17) has to be integrated from the center of the channel ($\eta = 1$) toward the wall. This results in

$$(U - U_0)/u_* = F(\eta), \tag{5.2.18}$$

where U_0 is the mean velocity at the center of the channel. We see that the appropriate similarity law for the core region is a *velocity-defect law*. Of course, (5.2.18) is not applicable as $\eta \to 0$.

Inertial sublayer A two-layer description as developed here requires special attention in the region where the two descriptions merge into each other. The existence of a *region of overlap* or *matched layer* is possible only if the limits $y_+ \to \infty$ and $\eta \to 0$ can be taken simultaneously. In Section 5.1 it was demon-

strated that this is possible if the Reynolds number is large enough (see Figure 5.1). More specifically, if $y_+ = cR_*^\alpha$, then $\eta = cR_*^{\alpha-1}$, so that $y_+ \to \infty$ and $\eta \to 0$ simultaneously if $0 < \alpha < 1$. This is called an *intermediate limit process*; it corresponds to travel toward the right on a straight line with slope $\alpha - 1$ in the plot given in Figure 5.3.

The process of obtaining the proper limiting behavior of the law of the wall and the velocity-defect law is called *asymptotic matching*. Formally, matching requires that the intermediate limits of the functions involved be equal for any α in the interval $0 < \alpha < 1$. However, in this particular case no such elegance is needed. Since we have demonstrated that an intermediate limit process is possible, we can now assume that the surface layer and the wall layer can be matched. It is most convenient to match the velocity gradients of the wall layer and the core region. According to (5.2.14), the velocity gradient in the surface layer is given by

$$\frac{dU}{dy} = \frac{u_*^2}{\nu}\frac{df}{dy_+}. \tag{5.2.19}$$

In the core region, (5.2.17) must be valid. Equating (5.2.17) and (5.2.19) and

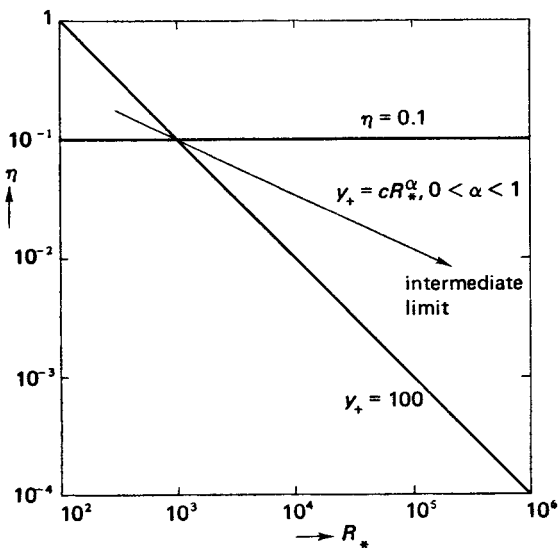

Figure 5.3. An intermediate limit process in which $y_+ \to \infty$ and $\eta \to 0$ simultaneously.

keeping in mind that we are considering some limit process in which $y_+ \to \infty$ and $\eta \to 0$ simultaneously, we obtain

$$\frac{u_*}{h}\frac{dF}{d\eta} = \frac{u_*^2}{\nu}\frac{df}{dy_+}. \tag{5.2.20}$$

On multiplication by y/u_*, this becomes

$$\eta\frac{dF}{d\eta} = y_+\frac{df}{dy_+} = \frac{1}{\kappa}. \tag{5.2.21}$$

The left-hand side of (5.2.21) can be a function only of η and the right-hand side can be a function only of y_+, because neither F nor f depends on any parameters. Thus, in the inertial sublayer both sides of (5.2.21) must be equal to the same universal constant. If the constant is denoted by $1/\kappa$, (5.2.21) can be integrated to yield

$$F(\eta) = \frac{1}{\kappa}\ln\eta + \text{const}, \tag{5.2.22}$$

$$f(y_+) = \frac{1}{\kappa}\ln y_+ + \text{const}. \tag{5.2.23}$$

Both of these are valid only if $\eta \ll 1$ and $y_+ \gg 1$.

The chain of arguments leading to (5.2.22, 5.2.23) was developed by Clark B. Millikan, who presented it at the Fifth International Congress of Applied Mechanics (Millikan, 1939). At that time, the formal theory of singular-perturbation problems was unknown; not until the decade 1950–1960 was a rational theory of multiple length-scale problems developed by Kaplun, Lagerstrom, Cole, and others (see Cole, 1968). The constant κ in (5.2.22, 5.2.23) is called von Kármán's constant, because Th. von Kármán was one of the first to derive the logarithmic velocity profile from similarity arguments (von Kármán, 1930).

The logarithmic velocity profile in the inertial sublayer is one of the major landmarks in turbulence theory. With analytical tools of a rather general nature a very specific result has been obtained, even though the equations of motion cannot be solved in general.

In this flow, matching of the Reynolds stress is straightforward. According to (5.2.12), $-\overline{uv}/u_*^2 \to 1$ if $\eta \to 0$. According to (5.2.13) and (5.2.21), for $y_+ \to \infty$,

$$-\overline{uv}/u_*^2 = 1 - 1/\kappa y_+, \tag{5.2.24}$$

so that

$$-\overline{uv}/u_*^2 \to 1 \text{ if } y_+ \to \infty. \tag{5.2.25}$$

The inertial sublayer thus is a region of approximately constant Reynolds stress. From (5.2.24) it is also clear that the viscous stress (which is proportional to the second term in (5.2.24)) is very small compared to the Reynolds stress if $y_+ >> 1$. The matched layer is called *inertial sublayer* because of this absence of local viscous effects.

Logarithmic friction law If (5.2.18) and (5.2.14) are substituted into (5.2.22) and (5.2.23), respectively, there results

$$\frac{U - U_0}{u_*} = \frac{1}{\kappa} \ln \eta + b, \tag{5.2.26}$$

$$\frac{U}{u_*} = \frac{1}{\kappa} \ln y_+ + a. \tag{5.2.27}$$

These expressions are valid only in the inertial sublayer. The constants a and b must be finite; they cannot depend on the Reynolds number $R_* = u_* h/\nu$ because f and F are independent of R_*. It follows from (5.2.26) and (5.2.27) that

$$\frac{U_0}{u_*} = \frac{1}{\kappa} \ln R_* + a - b, \tag{5.2.28}$$

because (5.2.26) and (5.2.27) must be valid simultaneously in the inertial sublayer. This relation is called the *logarithmic friction law*; it determines U_0 if the pressure gradient and the channel width are known.

Turbulent pipe flow Axisymmetric parallel flow in a circular pipe of constant diameter is of greater practical importance than plane channel flow. The geometry of pipe flow is sketched in Figure 5.4. We assume that the flow is *fully developed*, that is, independent of x. The origin of the y coordinate is put at the inner surface. This would be very inconvenient for most purposes, but it is convenient here, because we only need the mean-flow equation, which in these coordinates becomes

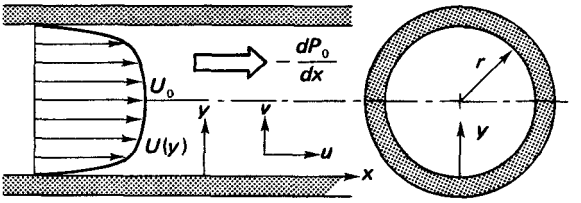

Figure 5.4. Definition sketch for pipe flow.

$$-\overline{uv} + \nu \frac{dU}{dy} = \frac{1}{2}(y - r)\frac{dP_0}{\rho dx}. \tag{5.2.29}$$

The derivation of (5.2.29) is left as an exercise for the reader. The momentum integral in fully developed pipe flow is, if the wall stress is again denoted by ρu_*^2,

$$2\pi r u_*^2 = \pi r^2 \frac{dP_0}{\rho dx}. \tag{5.2.30}$$

The momentum equation thus becomes

$$-\overline{uv} + \nu \frac{dU}{dy} = u_*^2 \left(1 - \frac{y}{r}\right), \tag{5.2.31}$$

which is identical to (5.2.6) if r is replaced by h. All of the conclusions obtained for channel flow thus apply equally to pipe flow. The shape of $F(\eta)$, where η now is defined as y/r, may be different from the shape of F in plane channel flow because of different geometrical constraints. However, the shape of $f(y_+)$ should be identical to that in plane channel flow, because the curvature of the wall is nearly zero if seen from points close enough to the surface to make y_+ finite.

Experimental data on pipe flow For turbulent flows in pipes with smooth walls, the logarithmic velocity profile and the logarithmic friction law are well represented by

$$U/u_* = 2.5 \ln y_+ + 5, \tag{5.2.32}$$

$$(U - U_0)/u_* = 2.5 \ln \eta - 1, \tag{5.2.33}$$

$$U_0/u_* = 2.5 \ln R_* + 6. \tag{5.2.34}$$

There is considerable scatter in the numerical constants; the values given represent averages over many experiments. In Section 5.4, we find that some of the "scatter" arises because no experiments have been performed at large enough Reynolds numbers. In particular, the logarithmic slope is probably very nearly 3 (instead of 2.5, which corresponds to the often-quoted $\kappa = 0.4$) if the Reynolds number $R_* = ru_*/\nu$ is large enough.

A volume-flow velocity U_b ("bulk" velocity) can be defined by

$$\pi r^2 U_b = \int_0^r 2\pi(r - y)U \, dy. \tag{5.2.35}$$

A fairly crude, but frequently used, approximation to the relation between U_b/u_* and R_* is

$$U_b/u_* = 2.5 \ln R_* + 1.5. \tag{5.2.36}$$

This relation has an interesting application. The local velocity $U(y)$ is equal to U_b at some point in the flow. If (5.2.32) and (5.2.36) are valid at that point, this occurs when

$$2.5 \ln r/y = 3.5, \tag{5.2.37}$$

which yields $y/r = \frac{1}{4}$. It so happens that in pipe flow the velocity profile follows (5.2.32) closely up to and somewhat beyond $\eta = \frac{1}{4}$, even though this is well outside the reach of the inertial sublayer. Thus, the volume flow through a smooth pipe can be determined simply by putting a small total-head probe at $\eta = \frac{1}{4}$ and drilling a static-pressure tap in the wall at the same value of x as that of the tip of the total-head tube. This is called a *quarter-radius probe*.

The viscous sublayer We now want to consider the law of the wall, (5.2.14, 5.2.15), in more detail. The first issue to be considered is whether or not the Reynolds stress can contribute to the stress at small values of y_+. At the surface itself, all of the stress is viscous stress. However, if the surface is rough and if $y = 0$ is taken at the mean height of the roughness elements, the shear stress at $y = 0$, as distinct from the shear stress at the surface, can be borne partly by the Reynolds stress if the roughness elements are large enough. We return to this issue later; for the moment, we restrict the discussion to flow over smooth surfaces.

It is useful to look at the problem from the point of view of the turbulence, rather than the mean flow, and to look from the inertial sublayer

downward toward the wall. In the inertial sublayer, the Reynolds stress is approximately equal to ρu^2, and the mean-velocity gradient is given by $u_*/\kappa y$. Hence, the turbulence production rate $-\overline{uv}\, dU/dy$ is equal to $u_*^3/\kappa y$. If turbulence production is mainly balanced by the viscous dissipation ϵ (experiments have shown that this is a fairly accurate statement in the inertial sublayer), we have

$$\epsilon \cong u_*^3/\kappa y. \tag{5.2.38}$$

The Kolmogorov microscale η (not easily confused with $\eta = y/r$ in this context) thus varies with y according to

$$\eta = \left(\frac{\nu^3}{\epsilon}\right)^{1/4} \cong \left(\frac{\kappa y \nu^3}{u_*^3}\right)^{1/4} = \kappa^{1/4} y\, y_+^{-3/4}. \tag{5.2.39}$$

The integral scale (ℓ) of the turbulence, on the other hand, must be of order y because the largest eddies should scale with the distance from the wall. In the inertial sublayer, $\partial U/\partial y = u_*/\kappa y$, so that $\ell \cong \kappa y$ is a suitable estimate. Non-dimensionally, we obtain

$$\eta_+ \equiv \eta u_*/\nu \cong (\kappa y_+)^{1/4}, \tag{5.2.40}$$

$$\ell_+ \equiv \ell u_*/\nu \cong \kappa y_+. \tag{5.2.41}$$

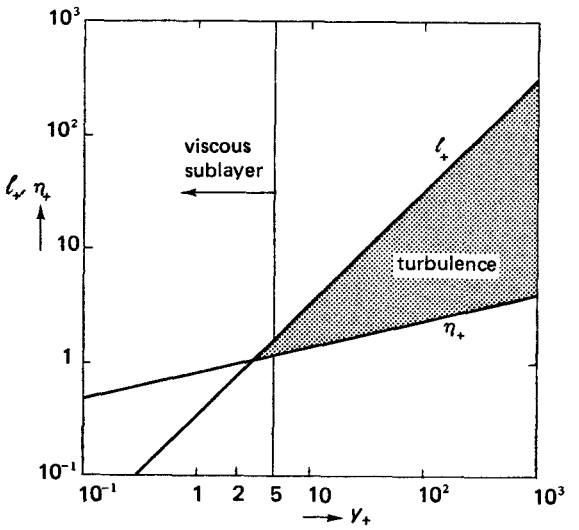

Figure 5.5. The variation of ℓ and η near the surface.

These relations are plotted in Figure 5.5; they show that the integral scale becomes smaller than the Kolmogorov microscale if y_+ is small. This is impossible, so that we must conclude that the turbulence cannot sustain itself and cannot generate Reynolds stresses if y_+ is small. Experimental evidence has shown that the Reynolds stress remains a small fraction of u_*^2 up to about $y_+ = 5$. This region is called the *viscous sublayer*. In the viscous sublayer, the flow is not steady, but the velocity fluctuations do not contribute much to the total stress because of the overwhelming effects of the viscosity. In some of the literature, the viscous sublayer is called the *laminar sublayer*; this name, however, is misleading because it suggests that no velocity fluctuations are present. In the viscous sublayer, the velocity profile must be linear ($U/u_* = y_+$), as indicated by the solution of (5.2.13) when $-\overline{uv}$ is neglected.

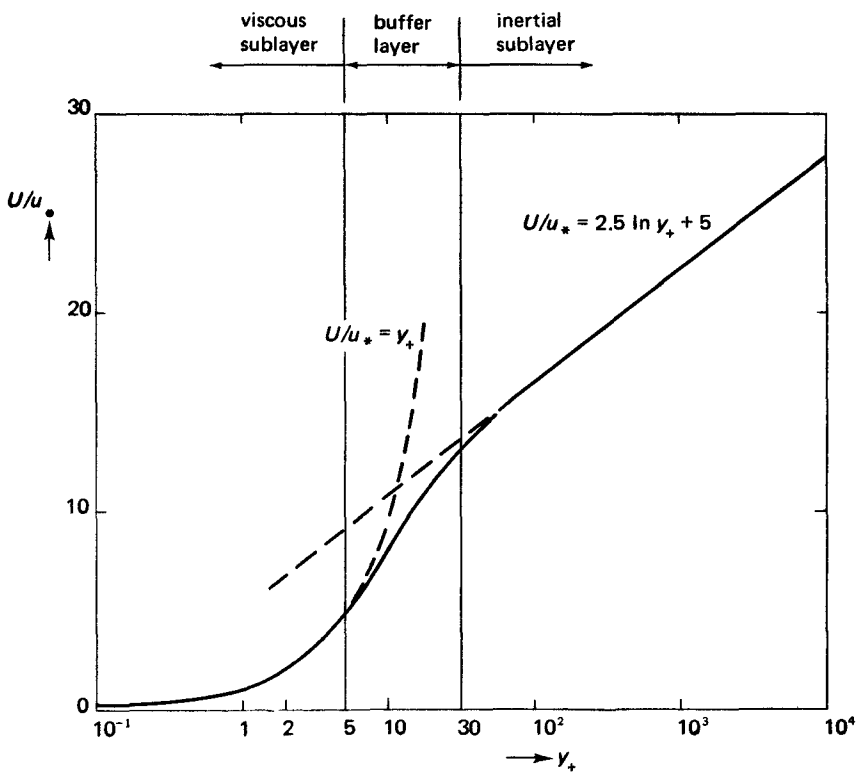

Figure 5.6. The law of the wall.

Experimental data on the law of the wall The velocity profile in the surface layer must satisfy $f = y_+$ for small y_+ and the logarithmic law (5.2.32) at large y_+. Experimentally obtained velocity profiles have the shape given in Figure 5.6. Another useful plot is the distribution of stresses. According to (5.2.13), the sum of the (nondimensionalized) viscous and Reynolds stresses must be equal to one throughout the surface layer. The two curves are sketched in Figure 5.7. The region where neither one of the stresses can be neglected is sometimes called the *buffer layer*. In many engineering calculations, the buffer layer is disposed of by linking the linear velocity profile in the viscous sublayer to the logarithmic velocity profile in the inertial sublayer. This causes an abrupt change from purely viscous stress to purely turbulent stress at $y_+ = 11$ approximately. The buffer layer is the site of vigorous turbulence dynamics, because the turbulent energy production rate $g\, df/dy_+$ reaches a maximum of $\frac{1}{4}$ at the value of y_+ where the Reynolds stress is equal to the viscous stress ($g = df/dy_+ = \frac{1}{2}$). This occurs at $y_+ = 12$ approximately, as is shown in Figure 5.7.

A few approximate numbers on the turbulence intensity in the surface layer may be useful. If the rms value of a variable is denoted by a prime, the

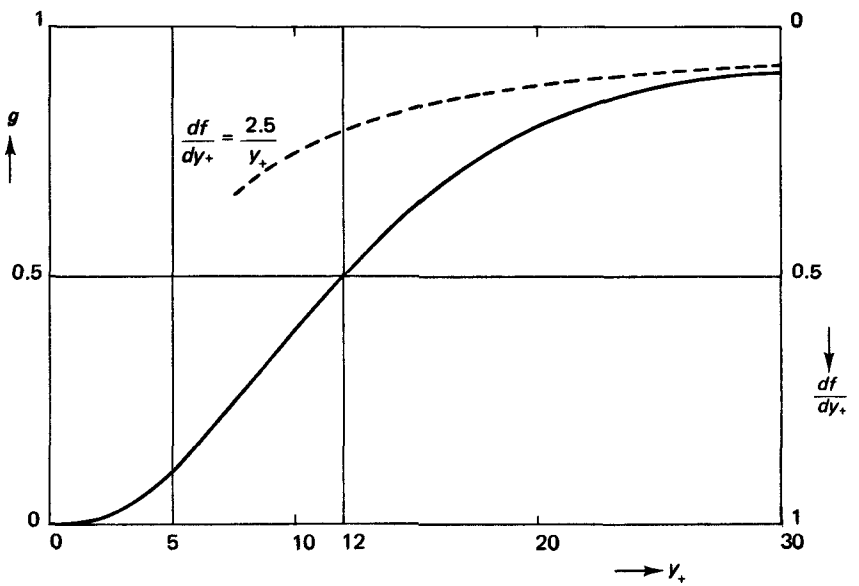

Figure 5.7. Distribution of Reynolds stress $g = -\overline{uv}/u_*^2$ and of viscous stress df/dy_+ in the surface layer (adapted from Hinze, 1959).

following relations hold in the inertial sublayer: $u' \cong 2u_*$, $v' \cong 0.8u_*$, $w' \cong 1.4u_*$, $\frac{1}{2}q^2 \cong 3.5u_*^2$, $-\overline{uv} \cong u_*^2 \cong 0.4\,u'v'$. The u component is largest because the turbulence-production mechanism favors it; the distribution of energy among the components is performed by nonlinear interaction.

Experimental data on the velocity-defect law A plot of the velocity-defect law is presented in Figure 5.8. In pipe flow, the logarithmic velocity profile (5.2.33) happens to represent the actual velocity profile fairly well all through the pipe, which is often quite convenient in engineering applications. The difference between the actual velocity profile in the core region and the logarithmic law, normalized by u_*, is called the *wake function* $W(\eta)$:

$$W(\eta) = 1 - 2.5 \ln \eta + F(\eta). \tag{5.2.42}$$

The wake function happens to be approximately sinusoidal in many wall-bounded flows; in this particular case, $W(\eta)$ is fairly well represented by

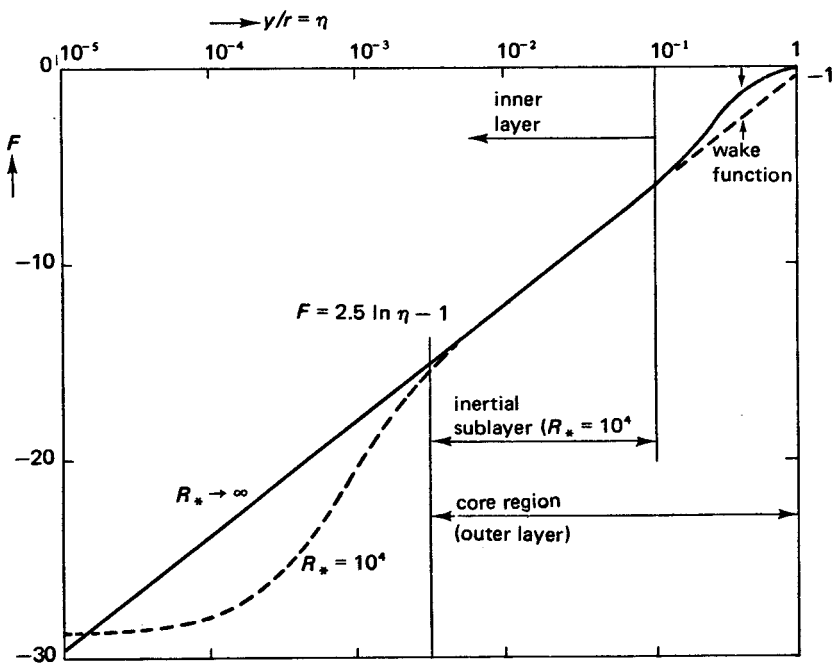

Figure 5.8. The velocity-defect law in pipe flow. The dashed curve on the left represents the actual velocity profile in the wall layer for $R_* = 10^4$. The width of the inertial sublayer increases with R_*.

$$W = \tfrac{1}{2}\,[\sin \pi\,(\eta - \tfrac{1}{2}) + 1]\,. \tag{5.2.43}$$

The amplitude of the sine wave is equal to $\frac{1}{2}$ in this case, but in boundary layers with opposing pressure gradients W can become quite large. The wake function W may be represented by a universal shape function $\mathscr{F}$ multiplied by a numerical constant that depends on the conditions of the flow. This representation is called the *law of the wake* because $\mathscr{F}$ is similar to the shape of the velocity-defect profile in wakes (Coles, 1956).

The turbulence intensity drops slowly if one goes from the surface toward the center. In the core region, a crude approximation to the experimental data is $u' = v' = w' \cong 0.8\,u_*$. The fluctuating velocity component v has a nearly constant amplitude across the pipe.

The flow of energy The surface layer is a "sink" for momentum, and therefore also for kinetic energy associated with the mean flow. Mean-flow kinetic energy transferred into the surface layer by Reynolds stresses is converted into turbulent kinetic energy (turbulence production) and into heat (viscous dissipation). If we integrate the transport term $\partial(\overline{uv}\,U)/\partial y$ between the surface and a value of y near the outer edge of the inertial sublayer, we conclude that the total loss of energy in that region is of order $\rho U_0 u_*^2$ per unit area and time, because U is fairly close to U_0 at the edge of the inertial sublayer. The direct loss to viscous dissipation occurs primarily in the viscous sublayer, because $\partial U/\partial y$ has a sharp peak at the surface. This loss is of order ρu_*^3: $\mu(\partial U/\partial y)^2$ is of order $\rho u_*^4/\nu$ in the viscous sublayer, but this loss is concentrated in a region whose height is only of order ν/u_*. Most of the mean-flow kinetic energy transported into the surface layer is thus used for the maintenance of turbulent kinetic energy.

In the core region, on the other hand, the Reynolds stress is of order ρu_*^2 and dU/dy is of order u_*/r. Integrating over the entire core region, the turbulence production per unit area and time in the core region is of order ρu_*^3. We conclude that most of the turbulence production occurs in the surface layer. The surface layer is the source of most of the turbulent energy. This conclusion must be viewed with caution, though, because the rate of dissipation of turbulent energy is also high in the surface layer.

The main function of the core region is not turbulence production, but transport of mean-flow kinetic energy into the surface layer. In the core of the pipe, the pressure gradient performs work at a rate of roughly $\rho u_*^2 U_0/r$

per unit volume and time. This energy input is carried off by the Reynolds stress to the surface layer, where it is converted into turbulent kinetic energy.

Flow over rough surfaces If the surface of a pipe or channel is rough, the arguments leading to the law of the wall require some modification. If the ratio k/r (k is an rms roughness height, say) is small enough, the roughness does not affect the velocity-defect law.

A definition sketch of flow over a rough surface is given in Figure 5.9. If $y = 0$ at the average vertical position at the surface, the velocity at $y = 0$ cannot be defined for a substantial fraction of the streamwise distance. As discussed earlier, the no-slip condition has to be satisfied at the surface, but the mean velocity obtained by averaging the instantaneous velocity at $y = 0$ over time and over all intervals Δx where the surface is below $y = 0$ need not be zero.

The surface layer over a rough wall has two characteristic lengths, k and ν/u_*, whose ratio is the roughness Reynolds number $R_k = ku_*/\nu$. We thus expect a law of the wall which can be written as

$$\frac{U}{u_*} = f_1(y_+, R_k), \tag{5.2.44}$$

or

$$\frac{U}{u_*} = f_2(y/k, R_k). \tag{5.2.45}$$

These expressions must be matched with the velocity-defect law. Because the latter is independent of roughness as long as $k/r \ll 1$ and because the matching is performed on the velocity derivative, the effects of roughness on

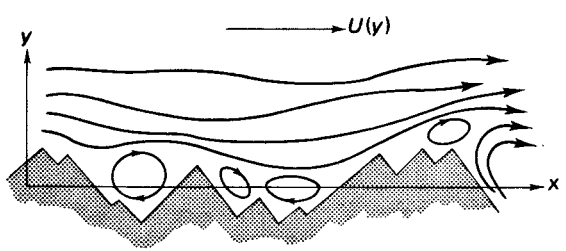

Figure 5.9. Flow over a rough surface.

the logarithmic velocity profile in the inertial sublayer can appear only as an additive function of the parameter:

$$\frac{U}{u_*} = \frac{1}{\kappa} \ln y_+ + f_3(R_k), \tag{5.2.46}$$

$$\frac{U}{u_*} = \frac{1}{\kappa} \ln \frac{y}{k} + f_4(R_k). \tag{5.2.47}$$

In the limit as $R_k \to 0$, f_3 has to become equal to 5, as comparison with (5.2.32) indicates. It turns out that roughness has no effect on (5.2.46) as long as $R_k < 5$, because the roughness elements are then submerged in the viscous sublayer in which no Reynolds stresses can be generated, however much the flow is disturbed.

For large values of R_k, a suitable nondimensional form of the equation of motion (5.2.31) is

$$-\frac{\overline{uv}}{u_*^2} + R_k^{-1} \frac{d(U/u_*)}{d(y/k)} = 1 - \frac{y}{k}\frac{k}{r}. \tag{5.2.48}$$

This shows that the viscous stress is very small at values of y/k of order one if $R_k \to \infty$. It should be noted that k/r must remain small, or else a distinct surface layer cannot exist. From (5.2.48) we conclude that $f_4(R_k)$ in (5.2.47) should be independent of R_k if it is large enough. This indeed occurs in practice for values of R_k above 30. The physical concept here is that roughness elements with large R_k generate turbulent wakes, which are responsible for essentially inviscid drag on the surface. For values of R_k between 5 and 30, the additive constant in the logarithmic part of the velocity profile (5.2.44, 5.2.45) depends on R_k.

The rough-wall velocity profile becomes, in the limit as $R_k \to \infty$,

$$\frac{U}{u_*} = \frac{1}{\kappa} \ln \frac{y}{k} + \text{const.} \tag{5.2.49}$$

Often, the position $y = 0$ is not known accurately enough to bother with the additive constant; instead, it is absorbed in the definition of k. Also, the logarithmic profile is often assumed to be valid all the way down to $y/k = 1$ (which makes $U = 0$ at $y/k = 1$ if the additive constant is ignored), even though its derivation was based on the limit process $y/k \to \infty$. The friction law corresponding to (5.2.49) is

$$\frac{U_0}{u_*} = \frac{1}{\kappa} \ln \frac{r}{k} + \text{const.} \tag{5.2.50}$$

5.3
Planetary boundary layers

The geostrophic wind The flow of air over the surface of the earth is affected by the Coriolis force that arises in any coordinate system that is rotating with respect to an inertial frame of reference. Under favorable conditions, the flow outside the boundary layer at the earth's surface is approximately steady, horizontal, and homogeneous in horizontal planes. In that case, the equations of motion reduce to a simple balance between pressure gradient and Coriolis forces. In the coordinate system of Figure 5.10, which is a Cartesian frame whose x, y plane is normal to the local vertical at latitude ϕ, this geostrophic balance is

$$-fV_g = -\frac{1}{\rho}\frac{\partial P}{\partial x}, \tag{5.3.1}$$

$$fU_g = -\frac{1}{\rho}\frac{\partial P}{\partial y}. \tag{5.3.2}$$

In these expressions U_g and V_g are the x and y components of the *geostrophic wind*, whose modulus is $G = (U_g^2 + V_g^2)^{1/2}$. The parameter f, which may be taken to be constant if the flow covers only a small range of latitudes

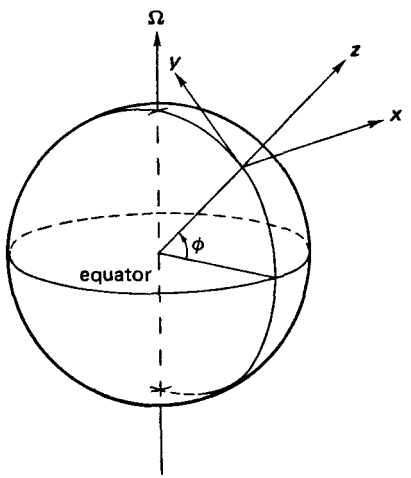

Figure 5.10. Coordinate system for planetary boundary layers.

ϕ, is equal to twice the z component of the angular velocity Ω at latitude ϕ:

$$f = 2\,\Omega \sin \phi. \tag{5.3.3}$$

This is called the *Coriolis parameter*. Its value is approximately $10^{-4}\,\mathrm{sec}^{-1}$ at $\phi = 40°$.

The Ekman layer The geostrophic wind does not meet the no-slip condition at the surface, so that a boundary layer must exist. If the flow in the boundary layer is steady and homogeneous in horizontal planes, the equations of motion for this planetary boundary layer, or *Ekman layer*, become

$$-f(V - V_g) = \frac{d}{dz}\,(-\overline{uw}), \tag{5.3.4}$$

$$f(U - U_g) = \frac{d}{dz}\,(-\overline{vw}). \tag{5.3.5}$$

Here, (5.3.1, 5.3.2) have been used to substitute for the pressure gradient. Also, it has been assumed that the roughness Reynolds number is so large that viscous stresses can be neglected. It is convenient to assume that the stress at the surface (ρu_*^2, by definition) has no y component, so that, for $z \to 0$,

$$-\overline{uw} = u_*^2, \quad -\overline{vw} = 0. \tag{5.3.6}$$

The velocity-defect law The equations of motion show quite clearly that a velocity-defect law is called for. We assume that u_* is the only characteristic velocity; this restricts us to flows in which no appreciable heat transfer occurs, because heat flux in a flow exposed to gravity may cause additional turbulence or may suppress turbulence, depending on its direction (see Chapter 3). The Reynolds stresses are presumably of order u_*^2, but the height h of the Ekman layer is unknown. A tentative nondimensional form of (5.3.4, 5.3.5) is thus

$$-\frac{fh}{u_*}\left(\frac{V - V_g}{u_*}\right) = \frac{d}{d(z/h)}\left(-\frac{\overline{uw}}{u_*^2}\right), \tag{5.3.7}$$

$$\frac{fh}{u_*}\left(\frac{U - U_g}{u_*}\right) = \frac{d}{d(z/h)}\left(-\frac{\overline{vw}}{u_*^2}\right). \tag{5.3.8}$$

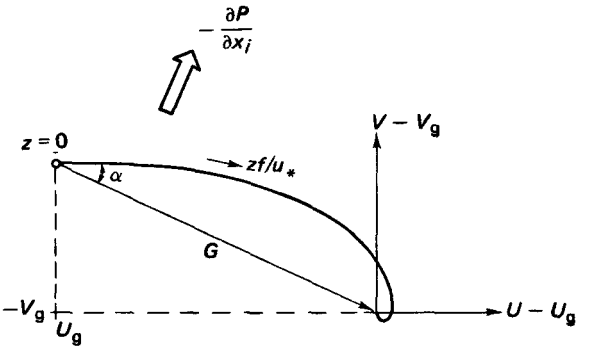

Figure 5.11. The Ekman velocity-defect spiral. The nondimensional height zf/u_* increases toward the right on the curve.

We are at liberty to select h for maximum convenience. If we choose

$$h = cu_*/f, \tag{5.3.9}$$

where c is some constant of order unity, the equations of motion become independent of any parameters, because all possible dependence has been absorbed by careful scaling. Thus, we expect that the velocity-defect law for Ekman layers should be (Blackadar and Tennekes, 1968)

$$(U - U_g)/u_* = F_u(zf/u_*), \tag{5.3.10}$$

$$(V - V_g)/u_* = F_v(zf/u_*). \tag{5.3.11}$$

Figure 5.11 shows a polar velocity plot of the experimentally observed defect law (5.3.10, 5.3.11) for the velocity vector in the Northern Hemisphere. The pressure-gradient vector is normal to the geostrophic wind, as (5.3.1) and (5.3.2) show. The Ekman spiral is located to the left of the geostrophic wind vector, because the Coriolis force in the boundary layer, where velocities are generally smaller than G, is insufficient to balance the pressure gradient. The angle between the surface wind (which is, as we shall see, parallel to the surface stress, that is, in the positive x direction) and the pressure gradient is thus less than 90°, so that the Ekman spiral rotates clockwise with increasing z.

The surface layer The Ekman spiral equations (5.3.10, 5.3.11) are not valid near the surface, because h is not the relevant length scale there. If the surface is rough, with a roughness height z_0 such that $z_0u_*/\nu \gg 1$, the relevant nondimensional form of (5.3.4, 5.3.5) is

$$-\frac{fz_0}{u_*^2}(V - V_g) = \frac{d(-\overline{uw}/u_*^2)}{d(z/z_0)}, \tag{5.3.12}$$

$$\frac{fz_0}{u_*^2}(U - U_g) = \frac{d(-\overline{vw}/u_*^2)}{d(z/z_0)}. \tag{5.3.13}$$

The left-hand sides of (5.3.12, 5.3.13) can be at most of order fz_0G/u_*^2. If we use (5.3.9), this can be written as z_0G/hu_*. For typical conditions in the atmosphere, $G/u_* \cong 30$, $h \cong 1{,}000$ m, $z_0 \cong 0.01$ m, so that $z_0G/hu_* \cong 3 \times 10^{-4}$. This is very small indeed. We shall neglect the left-hand sides of (5.3.12, 5.3.13); we shall shortly see that this is justified under the limit process which is involved. The surface layer, to first approximation, is thus a constant-stress layer which does not feel the turning effects of the Coriolis force. Because the stress at the surface has been assumed to have no y component, the wind in the surface also has no y component. The law of the wall must read

$$V/u_* = 0, \tag{5.3.14}$$

$$U/u_* = f_u(z/z_0). \tag{5.3.15}$$

These relations show that near the surface the wind is in the positive x direction, so that the Ekman spiral in Figure 5.11 must depart to the right horizontally from $U = 0$, $V = 0$. Also, because the spiral rotates clockwise, $V_g < 0$.

The logarithmic wind profile The law of the wall (5.3.14, 5.3.15) must be matched to the velocity-defect law (5.3.10, 5.3.11). This yields, where the usual procedures have been followed (Blackadar and Tennekes, 1968),

$$\frac{V_g}{u_*} = -F_v(0) = -A, \tag{5.3.16}$$

$$\frac{U}{u_*} = \frac{1}{\kappa}\ln\left(\frac{z}{z_0}\right) + B, \tag{5.3.17}$$

$$\frac{U - U_g}{u_*} = \frac{1}{\kappa}\ln\left(\frac{zf}{u_*}\right) + C, \tag{5.3.18}$$

$$\frac{U_g}{u_*} = \frac{1}{\kappa}\ln\left(\frac{u_*}{fz_0}\right) + B - C. \tag{5.3.19}$$

Here, (5.3.17) and (5.3.18) are valid only in the region where $z/z_0 \gg 1$ and $zf/u_* \ll 1$ simultaneously. The parameter u_*/fz_0 functions like a Reynolds number for the turbulent flow over smooth surfaces; it is called the *friction Rossby number*. The relations given above are asymptotic approximations, valid only for large enough friction Rossby numbers. From (5.3.16) and (5.3.19) we conclude that $fz_0G/u_*^2 \cong fz_0U_g/u_*^2 \cong (fz_0/u_*)\ln(u_*/fz_0)$, so that $fz_0G/u_*^2 \to 0$ as $u_*/fz_0 \to \infty$. The approximation involved in obtaining the law of the wall is indeed valid asymptotically.

The angle α between the wind in the surface layer and the geostrophic wind is given by (see Figure 5.11)

$$\tan\alpha = -V_g/U_g = Au_*/U_g = A/[(1/\kappa)\ln(u_*/fz_0) + B - C]. \tag{5.3.20}$$

Measurements suggest that $A \cong 12$, $C \cong 4$. The value of B is often set at zero, with a consequent minor change in z_0. If $B = 0$ and if z_0 and $1/\kappa$ are known, (5.3.17) can be used to determine the friction velocity u_* from a wind profile near the surface. This is a common practice because direct measurements of stress are quite difficult.

Ekman layers in the ocean The turbulent boundary layer near the surface of a body of water exposed to wind stresses is similar to the Ekman layer in the atmosphere, except for the boundary conditions. If there is no current at great depth and if pressure gradients may be neglected, the water current at the surface makes an angle α, given by the equivalent of (5.3.20), with respect to the stress at the surface. The polar plot of water currents in the Northern Hemisphere is given in Figure 5.12. The formal analysis of the problem is left to the reader.

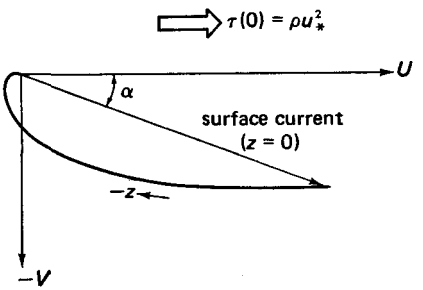

Figure 5.12. Ekman layer near the surface of the ocean (Northern Hemisphere).

5.4
The effects of a pressure gradient on the flow in surface layers

So far, we have encountered only surface layers in which the characteristic velocity is the friction velocity u_*. However, there exist conditions under which u_* is not appropriate. An interesting case is the surface layer of a boundary layer in which the stress at the wall is kept equal to zero for a considerable downstream distance by a carefully chosen distribution of an opposing pressure gradient. In engineering terms, such a boundary layer is on the verge of *separation*. Normally, this requires a rather large opposing pressure gradient, because Reynolds stresses can transfer momentum rapidly enough to prevent excessive deceleration in moderate pressure gradients.

The equations of motion, for steady two-dimensional flow, read

$$\frac{\partial U}{\partial x} + \frac{\partial V}{\partial y} = 0, \tag{5.4.1}$$

$$U\frac{\partial U}{\partial x} + V\frac{\partial U}{\partial y} = -\frac{1}{\rho}\frac{\partial P}{\partial x} - \frac{\partial}{\partial y}(\overline{uv}) - \frac{\partial}{\partial x}(\overline{u^2}) + \nu\frac{\partial^2 U}{\partial y^2} + \nu\frac{\partial^2 U}{\partial x^2}, \tag{5.4.2}$$

$$U\frac{\partial V}{\partial x} + V\frac{\partial V}{\partial y} = -\frac{1}{\rho}\frac{\partial P}{\partial y} - \frac{\partial}{\partial y}(\overline{v^2}) - \frac{\partial}{\partial x}(\overline{uv}) + \nu\frac{\partial^2 V}{\partial y^2} + \nu\frac{\partial^2 V}{\partial x^2}. \tag{5.4.3}$$

We use a coordinate system with a solid wall at $y = 0$. The mean flow in the half-plane $y \geqslant 0$ is in the positive x direction; the pressure gradient $\partial P/\partial x$ is positive. If the characteristic velocity in the surface layer is w, the length scale must be ν/w in order to preserve the viscous-shear stress in (5.4.2). We assume that U, u, and v scale with w, because no self-preservation can exist if the mean flow and the turbulence scale in different ways. The downstream length scale is L; we assume that $Lw/\nu >> 1$.

With $\partial U/\partial x \sim w/L$ and $\partial V/\partial y \sim Vw/\nu$, the continuity equation (5.4.1) gives $V \sim \nu/L$. The left-hand side of the y-momentum equation (5.4.3) is then of order $\nu w/L^2$. The orders of magnitude of the turbulence terms in (5.4.3) are

$$\partial(\overline{v^2})/\partial y = \mathcal{O}(w^3/\nu), \quad \partial(\overline{uv})/\partial x = \mathcal{O}(w^2/L); \tag{5.4.4}$$

the viscous terms in (5.4.3) are of order

$$\nu\,\partial^2 V/\partial y^2 = \mathcal{O}(w^2/L), \quad \nu\,\partial^2 V/\partial x^2 = \mathcal{O}(\nu^2/L^3). \tag{5.4.5}$$

Because $Lw/\nu >> 1$, the major turbulence term, $\partial(\overline{v^2})/\partial y$, must be balanced

by $\partial P/\rho\partial y$ to first order. Integration of this simplified equation with respect to y and differentiation with respect to x yields the familiar equation

$$\frac{1}{\rho}\frac{\partial P}{\partial x}+\frac{\partial \overline{v^2}}{\partial x}=\frac{1}{\rho}\frac{dP_0}{dx}. \tag{5.4.6}$$

Here, P_0 is the pressure at the surface ($y = 0$), which, of course, is not a function of y.

The various terms of (5.4.2) now may be estimated as follows:

$$\begin{aligned}
&(U\,\partial U/\partial x + V\,\partial U/\partial y) = \mathcal{O}(w^2/L),\\
&(1/\rho)(\partial P/\partial x - dP_0/dx) = \mathcal{O}(w^2/L),\\
&\partial(\overline{uv})/\partial y = \mathcal{O}(w^3/\nu), \quad \nu\,\partial^2 U/\partial y^2 = \mathcal{O}(w^3/\nu),\\
&\partial\,\overline{u^2}/\partial x = \mathcal{O}(w^2/L), \quad \nu\,\partial^2 U/\partial x^2 = \mathcal{O}(\nu w/L^2).
\end{aligned} \tag{5.4.7}$$

If $wL/\nu \gg 1$, only the shear-stress terms survive, while $\partial P/\partial x$ may be approximated by dP_0/dx. The approximate equation of motion is thus

$$\frac{\partial}{\partial y}\left(-\overline{uv}+\nu\frac{\partial U}{\partial y}\right)=\frac{1}{\rho}\frac{dP_0}{dx}. \tag{5.4.8}$$

Because P_0 is independent of y, this integrates to

$$-\overline{uv}+\nu\frac{\partial U}{\partial y}=\frac{y}{\rho}\frac{dP_0}{dx}. \tag{5.4.9}$$

Here, we have put the stress at the wall equal to zero, because that is the special case we want to consider. The pressure gradient now plays the role of an independent parameter, much like ρu_*^2 is treated as an independent parameter in other surface layers. Because we are considering a surface layer, the boundary-layer thickness δ and the downstream scale L are not relevant, so that a characteristic velocity has to be constructed with dP_0/dx and ν (the surface is smooth). The only possible choice is

$$u_p^3=\frac{\nu}{\rho}\frac{dP_0}{dx}. \tag{5.4.10}$$

The only parameter-free nondimensional form of (5.4.9) is

$$-\frac{\overline{uv}}{u_p^2}+\frac{\partial(U/u_p)}{\partial(yu_p/\nu)}=\frac{yu_p}{\nu}. \tag{5.4.11}$$

This equation has only one characteristic velocity (u_p) and one characteristic

length, and its boundary conditions are homogeneous (both U and the stress are zero at $y = 0$). Its solution must be a law of the wall of the form

$$U/u_p = f(yu_p/\nu), \tag{5.4.12}$$

$$-\overline{uv}/u_p^2 = g(yu_p/\nu). \tag{5.4.13}$$

The derivation of the corresponding velocity-defect law would carry us too far from the problem at hand. In first approximation, the flow in the outer part of these boundary layers is probably a pure "wake flow" in the sense that a wake function $W(y/\delta)$ like the one defined in (5.2.43), but with a peak-to-peak amplitude U_0, gives a good description of the first-order flow. At finite Reynolds numbers this wake flow is modified by a velocity-defect law that matches the law of the wall (5.4.12).

The mere existence of a velocity-defect law is all that needs to be assumed to predict that, at large yu_p/ν,

$$U/u_p = \alpha \ln yu_p/\nu + \beta. \tag{5.4.14}$$

This statement is supported by the observation that $\partial U/\partial y$ must be of order u_p/y if u_p is the only velocity scale in the problem and if $y >> \nu/u_p$. Experiments with a flow with zero wall stress were performed by Stratford (1959); his results suggest that $\alpha \cong 5$, $\beta \cong 8$. A sketch of the velocity profile is given in Figure 5.13.

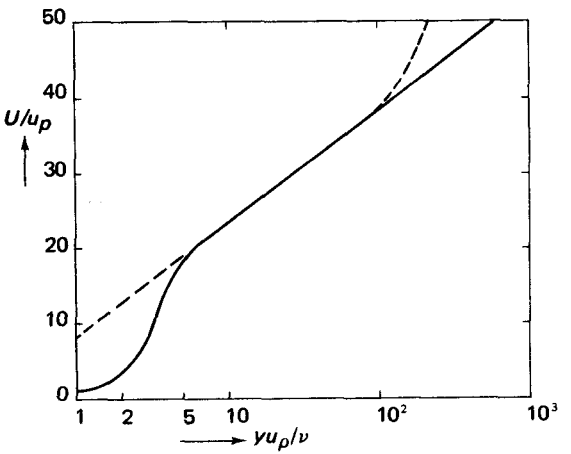

Figure 5.13. The surface layer in a flow with zero wall stress. The dashed curve at the right gives the velocity profile in the outer layer as it begins to deviate from the logarithm (based on data by Stratford, 1959).

A second-order correction to pipe flow The results obtained above suggest that it should be possible to estimate the effect of the pressure gradient on flows in other surface layers. Generally, pressure gradients are associated with acceleration or deceleration of the mean flow, so that their effects may be inseparable from nonlinear inertia effects. However, in pipe flows the inertia terms in the equation of motion vanish because of downstream homogeneity. Let us recall (5.2.29) and (5.2.30):

$$-\overline{uv} + \nu \frac{dU}{dy} = \frac{1}{2}(y - r)\frac{dP_0}{\rho dx}, \tag{5.4.15}$$

$$\frac{r}{\rho}\frac{dP_0}{dx} = -2u_*^2. \tag{5.4.16}$$

If we substitute for $r\,dP_0/dx$ with (5.4.16), the equation of motion becomes

$$-\overline{uv} + \nu \frac{dU}{dy} = u_*^2 + \frac{1}{2}\frac{y}{\rho}\frac{dP_0}{dx}. \tag{5.4.17}$$

The second term on the right-hand side of (5.4.17) is small in the surface layer, so that it is commonly neglected (see Section 5.2). In this particular case, there is no need to do so if we are willing to exploit the results obtained for the surface layer with zero wall stress.

We will think of the wall-layer flow and stress as consisting of two parts which add without interacting with each other. It can be shown that this is a valid procedure (Tennekes, 1968), but the formal proof requires multivariate asymptotic techniques, which are outside the scope of this book. The first-order flow and stress are associated with the constant stress ρu_*^2, and the second-order flow and stress are related to the small stress correction $\frac{1}{2}y\,dP_0/dx$. With these assumptions, we obtain the following system of equations:

$$U = U_1 + U_2, \tag{5.4.18}$$

$$-\overline{uv} = -(\overline{uv})_1 - (\overline{uv})_2, \tag{5.4.19}$$

$$-(\overline{uv})_1 + \nu \frac{dU_1}{dy} = u_*^2, \tag{5.4.20}$$

$$-(\overline{uv})_2 + \nu \frac{dU_2}{dy} = \frac{1}{2}\frac{y}{\rho}\frac{dP_0}{dx}. \tag{5.4.21}$$

The solution of (5.4.20) is the familiar law of the wall

$$U_1/u_* = f(yu_*/\nu), \tag{5.4.22}$$

which, at large $y_+ = yu_*/\nu$, behaves as

$$U_1/u_* = \frac{1}{\kappa} \ln y_+ + C. \tag{5.4.23}$$

The solution of (5.4.21) must be similar to the solution of (5.4.9), that is, it must be a law of the wall like (5.4.12). However, in pipe flow the pressure gradient is negative, so that U_2 is presumably also negative. The appropriate velocity scale for U_2 is u_{p2}, which is defined as

$$u_{p2}^3 = -\frac{\nu}{2\rho}\frac{dP_0}{dx}. \tag{5.4.24}$$

In this way, $u_{p2} > 0$. Nondimensionalized with u_{p2} and ν, (5.4.21) becomes

$$\frac{-(\overline{uv})_2}{u_{p2}^2} + \frac{d(U_2/u_{p2})}{d(yu_{p2}/\nu)} = -\frac{yu_{p2}}{\nu}. \tag{5.4.25}$$

This is identical to (5.4.11), except for the sign reversal in the total stress. The solution of (5.4.25) is thus identical to the solution of (5.4.11), except for a change of sign. This yields the counterpart of (5.4.12):

$$U_2/u_{p2} = -f(yu_{p2}/\nu). \tag{5.4.26}$$

In particular, for large yu_{p2}/ν,

$$U_2/u_{p2} = -\alpha \ln (yu_{p2}/\nu) - \beta. \tag{5.4.27}$$

According to (5.4.16) and (5.4.24), u_{p2} and u_* are related to each other by

$$u_{p2}^3 = u_*^3 \frac{\nu}{u_* r} = u_*^3 R_*^{-1}. \tag{5.4.28}$$

Hence, (5.4.27) can be written as

$$U_2/u_* = -\alpha R_*^{-1/3} \ln y_+ + h(R_*^{-1/3}), \tag{5.4.29}$$

where $h(R_*^{-1/3})$ contains all additive constants.

The slope of the logarithmic velocity profile There is too much experimental scatter in pipe-flow data to allow for a verification of all aspects of (5.4.29).

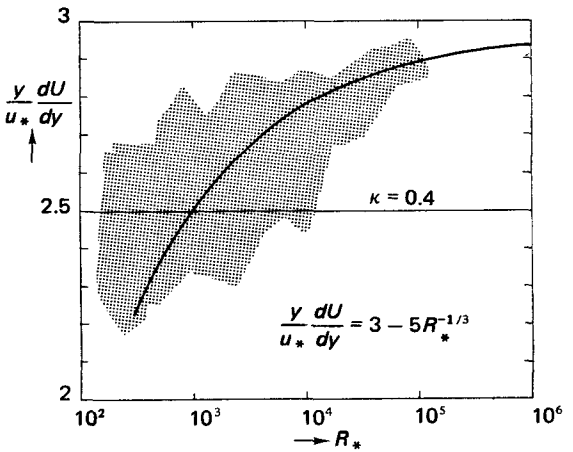

Figure 5.14. The slope of the velocity profile in pipe flow. The experimental scatter is indicated by the shaded area (adapted from Tennekes, 1968).

One major consequence of (5.4.29) is that the slope of the logarithmic velocity profile, in a region where $u_{p2}y/\nu \gg 1$, $u_*y/\nu \gg 1$, but $y/r \ll 1$, is a function of the Reynolds number R_*:

$$\frac{y}{u_*}\frac{dU}{dy} = \frac{y}{u_*}\left(\frac{dU_1}{dy} + \frac{dU_2}{dy}\right) = \frac{1}{\kappa} - \alpha R_*^{-1/3}. \tag{5.4.30}$$

The correction term is appreciable: if $R_* = 1{,}000$ and $\alpha \cong 5$, $\alpha R_*^{-1/3} \cong 0.5$, which is 20% of the value $1/\kappa = 2.5$ that is most often used. The asymptotic value of $1/\kappa$ must thus be about equal to 3. Experimental data (Figure 5.14) show that the trend predicted by (5.4.30) indeed exists.

The characteristic length for the second-order flow is ν/u_{p2}, which is larger than ν/u_* by a factor $R_*^{1/3}$. Therefore, the inertial sublayer of the second-order flow begins at a value of y much larger than the lower edge of the first-order inertial sublayer. It is instructive to look at this problem graphically. Figure 5.15 shows that the second-order inertial sublayer is substantially narrower than the first-order one. The limit lines in the figure are more or less arbitrary, but Figures 5.6 and 5.13 suggest that the respective flows are nearly inviscid for $y_+ > 30$ and $yu_{p2}/\nu > 10$, respectively.

If the asymptotic value of $1/\kappa$ is approximately 3 and if $\alpha \cong 5$, it takes an experiment at $R_* \cong 5 \times 10^6$ (which corresponds to $U_b r/\nu \cong 2 \times 10^8$) to

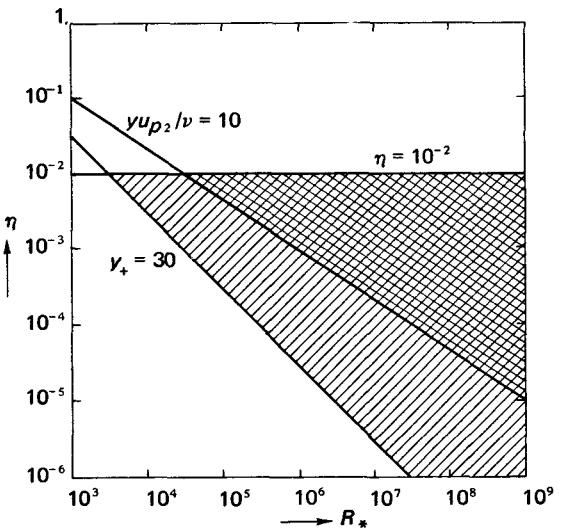

Figure 5.15. First-order and second-order inertial sublayers in pipe flow. Equation (5.4.30) should be valid in the crosshatched area.

determine $1/\kappa$ within 1% error. An experiment set up near a hydraulic power plant with a pipe of 4 m radius and water flowing at a velocity U_b = 50 m/sec would do the job. The pipe would have to be at least 1,000 m long in order to make sure that downstream homogeneity is achieved near the exit.

5.5
The downstream development of turbulent boundary layers

The thickness of boundary layers flowing over solid surfaces generally increases in the downstream direction, because the loss of momentum at the wall is diffused either by viscosity (molecular mixing) or by turbulent mixing. The growth of turbulent boundary layers, of course, is generally quite rapid compared to the growth of laminar boundary layers.

A general treatment of boundary-layer development under arbitrary boundary conditions is out of the question, because the equations of motion cannot be solved in general. Engineers who have to predict the development of a turbulent boundary layer on a wing or a ship's hull, say, use semiempirical techniques, such as described by Schlichting (1960). Here, we concentrate on a family of turbulent boundary layers in steady, plane flow in which

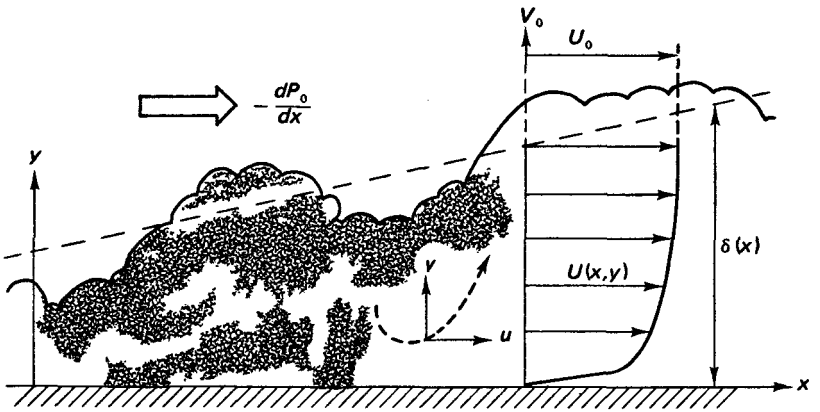

Figure 5.16. Definition sketch of plane boundary-layer flow.

the downstream pressure distribution is adjusted in such a way that their velocity profiles, if nondimensionalized with an appropriate velocity-defect law, are independent of the Reynolds number and of the downstream distance x. Such boundary layers are called *equilibrium layers*; they are equivalent to the Falkner-Skan family of laminar boundary layers.

We consider steady, incompressible, plane flows over a smooth surface without heat or mass transfer. A definition sketch is given in Figure 5.16; the equations of motion are

$$U\frac{\partial U}{\partial x}+V\frac{\partial U}{\partial y}=-\frac{1}{\rho}\frac{\partial P}{\partial x}+\frac{\partial}{\partial y}\left(-\overline{uv}+\nu\frac{\partial U}{\partial y}\right)+\frac{\partial}{\partial x}\left(-\overline{u^2}+\nu\frac{\partial U}{\partial x}\right), \tag{5.5.1}$$

$$U\frac{\partial V}{\partial x}+V\frac{\partial V}{\partial y}=-\frac{1}{\rho}\frac{\partial P}{\partial y}+\frac{\partial}{\partial y}\left(-\overline{v^2}+\nu\frac{\partial V}{\partial y}\right)+\frac{\partial}{\partial x}\left(-\overline{uv}+\nu\frac{\partial V}{\partial x}\right), \tag{5.5.2}$$

$$\frac{\partial U}{\partial x}+\frac{\partial V}{\partial y}=0. \tag{5.5.3}$$

The flow outside the boundary layer is assumed to be irrotational:

$$\frac{\partial U_0}{\partial y}-\frac{\partial V_0}{\partial x}=0. \tag{5.5.4}$$

A length scale L, associated with the rate of change of U_0 downstream, is defined by

$$\frac{1}{L} \equiv \left| \frac{1}{U_0} \frac{\partial U_0}{\partial x} \right|. \tag{5.5.5}$$

If the flow outside the boundary layer is uniform, $L \to \infty$. In that case, the distance x from a suitably defined origin is the appropriate length scale; the procedures used to obtain approximate equations of motion in that case are identical to those used for turbulent wakes. It turns out that the limit $L/x \to \infty$ does not cause any change or singularity in the first-order equations of motion, so that we can conveniently ignore the special case $L/x \to \infty$ in the analysis to follow.

We look for solutions to the equations of motion that satisfy a velocity-defect law,

$$(U - U_0)/u_* = F(y/\delta), \tag{5.5.6}$$

in such a way that F is independent of the downstream distance x. In other words, we are looking for *self-preserving* flows. Of course, the self-preserving solutions should be asymptotically independent of Reynolds number, so that they can describe an entire family of flows, in which a suitably nondimensionalized pressure gradient is the only parameter. The velocity-defect law (5.5.6) is not expected to be valid in the surface layer, so that the latter must be treated separately.

From the experience gained with pipe flow we can safely assume that $u_*/U_0 \ll 1$ if the Reynolds number $\delta u_*/\nu$ is made sufficiently large. This implies that the shear stress at the wall, ρu_*^2, is very small compared to ρU_0^2. We also assume that the boundary layer grows fairly slowly: $\delta/L \ll 1$ and $\delta/x \ll 1$. All of these assumptions will have to be justified a posteriori.

The potential flow The flow outside the boundary layer is governed by

$$U_0 \frac{\partial U_0}{\partial x} + V_0 \frac{\partial U_0}{\partial y} = -\frac{1}{\rho} \frac{\partial P_0}{\partial x}, \tag{5.5.7}$$

$$U_0 \frac{\partial V_0}{\partial x} + V_0 \frac{\partial V_0}{\partial y} = -\frac{1}{\rho} \frac{\partial P_0}{\partial y}, \tag{5.5.8}$$

together with the appropriate continuity equation and (5.5.4).

With (5.5.6), the continuity equation (5.5.3) may be written as

$$\frac{\partial V}{\partial y} = -\frac{\partial U_0}{\partial x} - \frac{\partial}{\partial x}(u_* F). \tag{5.5.9}$$

Now, the length scale associated with changes in the potential flow is L, so that $\partial U_0/\partial x$ is essentially constant over a distance δ if $\delta/L \ll 1$. Treating $\partial U_0/\partial x$ as a constant, we obtain by integrating (5.5.9) from $y = 0$ to $y = \delta$:

$$V_0(\delta) = -\delta \frac{\partial U_0}{\partial x} - \frac{d}{dx}(u_*\delta) \int_0^\delta F \, d\eta. \tag{5.5.10}$$

Here, $V_0(\delta)$ is the value of V_0 just outside the boundary layer. If the integral in (5.5.10) is finite and if $u_* \ll U_0$, (5.5.10) may be approximated by

$$V_0(\delta) = -\delta \frac{\partial U_0}{\partial x}. \tag{5.5.11}$$

This equation is not valid if $\partial U_0/\partial x$ is very small, as it would be if the pressure gradient $\partial P_0/\partial x$ were small. In that case, the approximations developed for turbulent wakes should be used.

Differentiating the condition of zero vorticity (5.5.4) with respect to x, we estimate

$$\frac{L}{U_0}\frac{\partial}{\partial y}\left(\frac{\partial U_0}{\partial x}\right) = \frac{L}{U_0}\frac{\partial^2 V_0}{\partial x^2} = \mathcal{O}\left(\frac{\delta}{L^2}\right). \tag{5.5.12}$$

This shows that the relative change of $\partial U_0/\partial x$ over a distance δ is of order $(\delta/L)^2$, so that $\partial U_0/\partial x$ can indeed be treated as a constant as far as the boundary layer is concerned.

From (5.5.4) and (5.5.11) we find that $\partial U_0/\partial y = \partial V_0/\partial x = \mathcal{O}(\delta U_0/L^2)$. We can now estimate the left-hand side terms of (5.5.7, 5.5.8) just outside the boundary layer. The result is

$$U_0 \frac{\partial U_0}{\partial x} = \mathcal{O}\left(\frac{U_0^2}{L}\right), \quad V_0 \frac{\partial U_0}{\partial y} = \mathcal{O}\left(\frac{\delta^2 U_0^2}{L^3}\right), \tag{5.5.13}$$

$$U_0 \frac{\partial V_0}{\partial x} = \mathcal{O}\left(\frac{\delta U_0^2}{L^2}\right), \quad V_0 \frac{\partial V_0}{\partial y} = \mathcal{O}\left(\frac{\delta U_0^2}{L^2}\right). \tag{5.5.14}$$

If $\delta/L \ll 1$, $\partial P_0/\partial y \ll \partial P_0/\partial x$, because both terms of (5.5.8) are of the same order and both are a factor δ/L smaller than the dominant term of (5.5.7). This implies that the entire equation for V_0 is dynamically insignificant. The second term on the left-hand side of (5.5.7) is of order δ^2/L^2 compared to the first. If $\delta/L \ll 1$, the equations for the inviscid flow above the boundary layer may thus be approximated by the single equation

$$U_0 \frac{dU_0}{dx} = -\frac{1}{\rho}\frac{dP_0}{dx}. \tag{5.5.15}$$

No partial derivatives are needed to this approximation, because U_0 and P_0 are essentially independent of y as far as the boundary layer is concerned.

The pressure inside the boundary layer We now estimate the order of magnitude of all terms in (5.5.2). If the Reynolds number is large enough, viscous stresses are small compared to Reynolds stresses, so that we may write

$$U\frac{\partial V}{\partial x} + V\frac{\partial V}{\partial y} = -\frac{1}{\rho}\frac{\partial P}{\partial y} - \frac{\partial \overline{v^2}}{\partial y} - \frac{\partial \overline{uv}}{\partial x}. \tag{5.5.16}$$

Since the velocity defect is small, U is of order U_0. The order of magnitude of V is $V_0(\delta)$, which is equal to $\delta U_0/L$. Thus, $U\,\partial V/\partial x = \mathcal{O}(\delta U_0^2/L^2)$. The gradient $\partial V/\delta y = \mathcal{O}(V_0/\delta)$, so that $V\,\partial V/\partial y = \mathcal{O}(\delta U_0^2/L^2)$. The Reynolds stress terms are $\partial\overline{v^2}/\partial y = \mathcal{O}(u_*^2/\delta)$ and $\partial\overline{uv}/\partial x = \mathcal{O}(u_*^2/L)$. The last two estimates are based on the assumption that the stress is of order ρu_*^2 throughout the boundary layer, so that u_* is the relevant velocity scale for the turbulent motion. This assumption is not valid if the pressure gradient causes separation, as we have seen in Section 5.4.

The second Reynolds-stress term in (5.5.16) may be neglected compared to the first. An approximate integral of (5.5.16) then reads

$$\frac{P_0}{\rho} - \frac{P}{\rho} = \overline{v^2} - \int_y^\delta \left(U\frac{\partial V}{\partial x} + V\frac{\partial V}{\partial y}\right) dy. \tag{5.5.17}$$

The first term on the right-hand side of (5.5.17) is of order u_*^2 and the integral is of order $(\delta U_0/L)^2$. These two terms are of the same order of magnitude if γ, defined by

$$\gamma \equiv u_* L/U_0\delta, \tag{5.5.18}$$

is finite. This amounts to $u_*/U_0 = \mathcal{O}(\delta/L)$, which is similar to the scale relation used in wakes. We assume, subject to later verification, that γ indeed is of order one. Differentiating (5.5.17), we obtain

$$\frac{1}{\rho}\frac{\partial P}{\partial x} - \frac{1}{\rho}\frac{dP_0}{dx} = \mathcal{O}\left(\frac{u_*^2}{L}\right). \tag{5.5.19}$$

The boundary-layer equation With these results, the boundary-layer approximation to (5.5.1) can be obtained. The approximation has to be performed rather carefully, because (5.5.1) is dominated by $U\,\partial U/\partial x$ and $\partial P/\rho\partial x$, both of which are of order U_0^2/L. We are looking for flows which satisfy the velocity-defect law (5.5.6), so that the following decomposition is useful:

$$U\frac{\partial U}{\partial x} = U_0\frac{dU_0}{dx} + U_0\frac{\partial}{\partial x}(U-U_0) + (U-U_0)\frac{dU_0}{dx} + (U-U_0)\frac{\partial}{\partial x}(U-U_0). \tag{5.5.20}$$

The first term on the right-hand side of (5.5.20) cancels the pressure gradient by virtue of (5.5.15). If F is finite, the next two terms are of order U_0u_*/L; it is clear that these should be retained. However, terms of order u_*^2/L can be neglected. The difference between $\partial P/\rho\partial x$ and $dP_0/\rho dx$ is of order (u_*^2/L), as (5.5.19) shows, so that $\partial P/\partial x$ can be replaced by dP_0/dx. The stress term $\partial\overline{u^2}/\partial x = \mathcal{O}(u_*^2/L)$ can be neglected for the same reason. The viscous term $\nu\partial^2U/\partial x^2 = \mathcal{O}(\nu U_0/L^2) = \mathcal{O}(u_*^2/L)(\nu/u_*\delta)$ if $U_0/u_* = \mathcal{O}(L/\delta)$ (5.5.18), so that it also can be neglected if $u_*\delta/\nu$ is not small.

On basis of the results obtained so far, (5.5.1) may be approximated by

$$U_0\frac{\partial}{\partial x}(U-U_0) + (U-U_0)\frac{dU_0}{dx} + (U-U_0)\frac{\partial}{\partial x}(U-U_0) + V\frac{\partial}{\partial y}(U-U_0$$

$$= \frac{\partial}{\partial y}\left(-\overline{uv} + \nu\frac{\partial U}{\partial y}\right). \tag{5.5.21}$$

The last term on the left-hand side could be written in terms of the velocity defect because U_0 is independent of y. The assumption that the velocity defect $(U_0 - U)$ is of order u_* has not yet been applied to the left-hand side of this equation. Because the velocity defect is not small in the surface layer and because the surface stress is purely viscous, further simplification of (5.5.21) should be delayed until a momentum integral has been obtained.

Before we do this, let us look at the orders of magnitude of the various terms in (5.5.21). The Reynolds-stress term in (5.5.21) is of order u_*^2/δ. The first and second terms on the left-hand side of (5.5.21) are of order U_0u_*/L. The Reynolds-stress term, therefore, is of order $u_*L/\delta U_0 = \gamma$ compared to the major inertia terms. Three limit processes are possible. If $\gamma \to 0$ as $\delta u_*/\nu \to \infty$, Reynolds stresses are negligible. This corresponds to situations with extremely rapid acceleration or deceleration of the flow; the particular limit process involved is sometimes used to compute the initial reaction of

turbulent boundary layers to very rapid changes in pressure. If $\gamma \to \infty$, the inertia terms are small compared to the Reynolds stresses. Physically speaking, this is an impossible situation; it corresponds to a Reynolds stress which is independent of y, and therefore equal to zero (because the stress must be zero outside the boundary layer).

The *distinguished limit* is clearly the case in which γ remains finite, no matter how large the Reynolds number is. This is a significant conclusion, because it implies that equilibrium flows can be obtained only if the ratio of the turbulence time scale δ/u_* to the flow time scale L/U_0 is finite and remains constant as the boundary layer develops. In other words, the boundary-layer turbulence has to keep pace with the flow.

Let us return to the momentum integral. Rearranging (5.5.21) with help of the continuity equation (5.5.3), we obtain

$$\frac{\partial}{\partial x}[U(U-U_0)] + \frac{\partial}{\partial y}[V(U-U_0)] + (U-U_0)\frac{dU_0}{dx} = \frac{\partial}{\partial y}\left(-\overline{uv} + \nu\frac{\partial U}{\partial y}\right). \tag{5.5.22}$$

Integration of (5.5.22) yields

$$-\frac{d}{dx}\int_0^\infty U(U-U_0)\,dy - \frac{dU_0}{dx}\int_0^\infty (U-U_0)\,dy = u_*^2. \tag{5.5.23}$$

As before, the stress at the surface is defined as ρu_*^2. Outside the boundary layer, the stress and the velocity defect are zero. The exact location of the upper limit of the integrals in (5.5.23) is immaterial; the infinity symbol is merely used for convenience.

A *normalized boundary-layer thickness* Δ may be defined by

$$\Delta u_* \equiv \int_0^\infty (U_0 - U)\,dy. \tag{5.5.24}$$

If $U_0 - U$ is of order u_* through most of the boundary layer, Δ and δ are of the same order of magnitude. Using (5.5.24), we can write the first integral in (5.5.23) as

$$-\int_0^\infty U(U-U_0)\,dy = U_0 u_* \Delta - \int_0^\infty (U-U_0)^2\,dy. \tag{5.5.25}$$

If the velocity defect is small, the last integral in (5.5.25) is of order $u_*^2\Delta$. In the surface layer, however, $U - U_0 \sim U_0$, so that the contribution to the last

integral made in the surface layer is of order $U_0^2\nu/u_*$ (the thickness of the surface layer is of order ν/u_*). Therefore, it is of order $(U_0/u_*)^2$ $(\nu/u_*\Delta)$ relative to the contribution made by the rest of the boundary layer. Because we expect that $U_0/u_* \to \infty$ much slower than $\Delta u_*/\nu$, this contribution can be neglected. Finally, because $u_*/U_0 \ll 1$, only the first term on the right-hand side of (5.5.25) needs to be retained in first approximation. Therefore, (5.5.23) may be approximated by

$$\frac{d}{dx}(\Delta u_* U_0) + \Delta u_* \frac{dU_0}{dx} = u_*^2. \tag{5.5.26}$$

We can now return to (5.5.21). Outside the surface layer, the viscous term can be neglected if $\delta u_*/\nu$ is large. The third inertia term is of order u_*^2/L if the velocity defect is of order u_*, so that it is small compared to the leading terms. The cross-stream velocity component V occurs in (5.2.21); if the analysis leading from (5.5.9) to (5.5.11) is repeated with an arbitrary upper limit of integration, there results $V = -y\,dU_0/dx$ with a correction term that can be neglected if $u_*/U_0 \ll 1$. The equation of motion for the outer layer thus becomes

$$U_0 \frac{\partial}{\partial x}(U - U_0) + (U - U_0)\frac{dU_0}{dx} - y\frac{dU_0}{dx}\frac{\partial}{\partial y}(U - U_0) = -\frac{\partial \overline{uv}}{\partial y}. \tag{5.5.27}$$

This equation is linear in the velocity defect $U_0 - U$; it is called the *linearized boundary-layer equation.*

Equilibrium flow We want to find solutions to (5.5.27) which satisfy

$$(U - U_0)/u_* = F(\eta), \tag{5.5.28}$$

$$-\overline{uv}/u_*^2 = G(\eta), \tag{5.5.29}$$

where

$$\eta = y/\Delta. \tag{5.5.30}$$

The normalized boundary-layer thickness Δ has been used here for convenience. Substitution of (5.5.28) and (5.5.29) into (5.5.27) yields

$$\frac{\Delta}{u_*^2}\frac{d}{dx}(U_0 u_*)F - \frac{1}{u_*}\frac{d}{dx}(\Delta U_0)\,\eta\frac{dF}{d\eta} = \frac{dG}{d\eta}. \tag{5.5.31}$$

If the coefficients in this equation can be made independent of x, the equa-

tion of motion allows self-preserving solutions. However, further analysis of (5.5.31) cannot proceed until the equations for the wall layer have been examined.

The flow in the wall layer Let us consider the equation for U in the immediate vicinity of the surface. We expect U to be of order u_*, so that $U\,\partial U/\partial x$ is of order u_*^2/L. Also, $\partial U/\partial x = \mathcal{O}(u_*/L)$, so that $V = \mathcal{O}(\nu/L)$ if ν/u_* is the length scale for the wall layer. Hence, $V\,\partial U/\partial y = \mathcal{O}(u_*^2/L)$. The pressure-gradient term is of order U_0^2/L, so that the inertia terms should be neglected if $u_*/U_0 \ll 1$. The length scale in the wall layer is ν/u_* in order to keep Reynolds stress and viscous stress of the same order of magnitude. The leading stress terms in the equation for U are $\partial\overline{uv}/\partial y$ and $\nu\,\partial^2 U/\partial y^2$; they are of order u_*^3/ν. The pressure gradient is of order $\nu U_0^2/Lu_*^3$ compared to the other stress terms. Now,

$$\frac{\nu U_0^2}{Lu_*^3} = \frac{U_0\delta}{u_*L}\cdot\frac{U_0}{u_*}\cdot\frac{\nu}{u_*\delta}. \tag{5.5.32}$$

The first factor on the right-hand side of (5.5.32) is $1/\gamma$. Because we decided not to deal with very rapidly accelerating or decelerating flows, γ is finite. As was stated before, $U_0/u_* \to \infty$ rather slowly compared to $\delta u_*/\nu$. Therefore, the pressure gradient is small compared to the principal Reynolds-stress and viscous-stress terms in the inner layer. The equation of motion reduces to

$$0 = \frac{\partial}{\partial y}\left(-\overline{uv} + \nu\frac{\partial U}{\partial y}\right). \tag{5.5.33}$$

It can be seen intuitively that this approximation is correct. Throughout the analysis, it has been assumed that the velocity defect is of order u_* and that Reynolds stresses are of order ρu_*^2. These assumptions can be valid only if no other characteristic velocity is relevant. In conditions where the pressure gradient might generate a new velocity scale (like the one used in Section 5.4), the obvious requirement is that it be small compared to the friction velocity u_*.

The law of the wall Equation (5.5.33) defines a constant-stress layer with wall stress ρu_*^2. The nature of the solutions of (5.5.33) has been studied in Section 5.2; we recall that

$$U/u_* = f(yu_*/\nu), \tag{5.5.34}$$

$$-\overline{uv}/u_*^2 = g(yu_*/\nu). \tag{5.5.35}$$

To first approximation the flow in the wall layer is independent of the pressure gradient. This result was first discovered in experiments made by Ludwieg and Tillmann (1949).

The logarithmic friction law We assume that solutions to the equation of motion for the outer layer which satisfy the velocity-defect law (5.5.28) do exist. If this is the case, the law of the wall (5.5.34) must be matched to the velocity-defect law (5.5.28) through a logarithmic velocity profile. The logarithmic velocity profile gives a logarithmic friction law, which may be written as

$$\frac{U_0}{u_*} = \frac{1}{\kappa} \ln \frac{\Delta u_*}{\nu} + A. \tag{5.5.36}$$

The additive constant A can be a function of a pressure-gradient parameter. For later use, a differentiated form of (5.5.36) is given. A convenient form is

$$\left(1 + \frac{u_*}{\kappa U_0}\right) \frac{d}{dx}\left(\frac{U_0}{u_*}\right) = \frac{1}{\kappa \Delta} \frac{d\Delta}{dx} + \frac{1}{\kappa U_0} \frac{dU_0}{dx}. \tag{5.5.37}$$

The pressure-gradient parameter We now determine under what conditions self-preserving solutions to (5.5.31) may be expected. The coefficients occurring in (5.5.31) may be expanded as follows:

$$\frac{\Delta}{u_*^2} \frac{d}{dx}(U_0 u_*) = 2 \frac{\Delta}{u_*} \frac{dU_0}{dx} + \frac{\Delta U_0^2}{u_*^2} \frac{d}{dx}\left(\frac{u_*}{U_0}\right), \tag{5.5.38}$$

$$\frac{1}{u_*} \frac{d}{dx}(\Delta U_0) = \frac{U_0}{u_*^2} \frac{d}{dx}(\Delta u_*) - \frac{\Delta U_0^2}{u_*^2} \frac{d}{dx}\left(\frac{u_*}{U_0}\right). \tag{5.5.39}$$

The momentum integral (5.5.26) may be rearranged to read

$$\frac{U_0}{u_*^2} \frac{d}{dx}(\Delta u_*) = 1 - 2 \frac{\Delta}{u_*} \frac{dU_0}{dx}. \tag{5.5.40}$$

Substitution of the differential friction law (5.5.37) into (5.5.38, 5.5.39) shows that the last terms of (5.5.38) and (5.5.39) are small compared to the others if $u_*/U_0 \ll 1$. Inspection of the set (5.5.38, 5.5.39, 5.5.40) then indicates that a convenient pressure-gradient parameter is Π, defined by

$$\Pi \equiv -\frac{\Delta}{u_*}\frac{dU_0}{dx}. \tag{5.5.41}$$

This result is not surprising: self-preservation can be obtained only if the ratio of the time scales $(dU_0/dx)^{-1}$ and Δ/u_* is a constant (see the discussion following (5.5.21) and (5.5.56)).

In terms of Π, (5.5.31) and (5.5.40) read

$$-2\Pi F - (1 + 2\Pi)\,\eta\frac{dF}{d\eta} = \frac{dG}{d\eta}, \tag{5.5.42}$$

$$\frac{U_0}{u_*^2}\frac{d}{dx}(\Delta u_*) = 1 + 2\Pi. \tag{5.5.43}$$

The system (5.5.36, 5.5.42, 5.5.43) is subject to a normalization condition imposed by the definitions (5.5.24) and (5.5.28) of Δ and F, respectively. The normalization condition is

$$\int_0^\infty F\,d\eta = -1. \tag{5.5.44}$$

The boundary conditions imposed on (5.5.42) are

$$F \to 0, G \to 0 \quad \text{for } \eta \to \infty, \tag{5.5.45}$$

$$G \to 1 \quad \text{for } \eta \to 0, \tag{5.5.46}$$

$$\eta\,dF/d\eta \to 1/\kappa \quad \text{for } \eta \to 0. \tag{5.5.47}$$

The system of equations (5.5.36, 5.5.42–5.5.47) is independent of x if Π is a constant. Therefore, we may expect self-preserving boundary-layer flows in pressure distributions that make Π independent of x. The problem defined by (5.5.42–5.5.47) is also independent of the Reynolds number, so that the solutions $F(\eta)$, $G(\eta)$ exhibit asymptotic invariance (Reynolds-number similarity). Therefore, boundary layers in which Π is constant are *equilibrium layers*; their velocity profiles are self-preserving and the velocity profiles of two different boundary layers at the same value of Π are identical, even if their Reynolds numbers are not the same. Of course, all of these statements are only valid asymptotically as $\Delta u_*/\nu \to \infty$.

These conclusions were first obtained by F. H. Clauser (1956). Clauser performed a series of experiments in which the pressure distribution was carefully adjusted in order to obtain downstream invariance of the velocity-defect function $F(\eta)$. His experiments showed that the pressure distribution

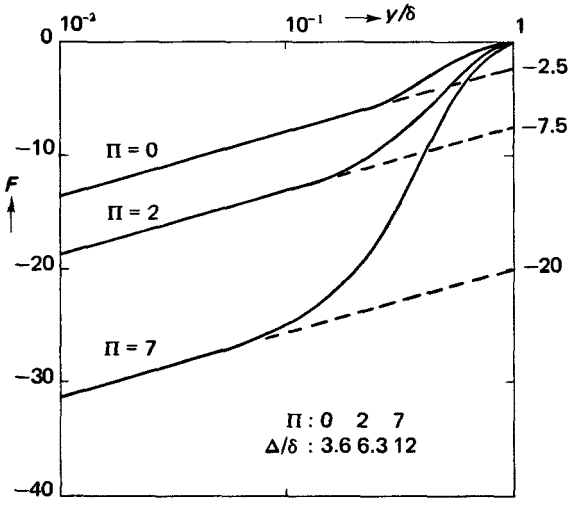

Figure 5.17. Velocity-defect profiles at different values of Π. The scaling length for y is the boundary-layer thickness δ, defined as the value of y where $F = -0.1$ (based on data by Clauser, 1956).

was well represented by a constant value of Π. The significance of Π was discovered from an ad hoc argument involving the relative contributions of the wall stress and the pressure gradient to the rate of increase of momentum deficit in the boundary layer.

Some of the velocity profiles obtained by Clauser and others for different values of Π are shown in Figure 5.17. The additive constant in the logarithmic part of F increases rapidly with Π; the amplitude of the wake function $W(\eta)$, which is the difference between F and its logarithmic part, therefore also increases with Π. In the limit $\Pi \to \infty$, the velocity profile may be a pure wake function.

Free-stream velocity distributions The equations governing the downstream development of equilibrium layers (5.5.41, 5.5.43, 5.5.36) are

$$\frac{\Delta}{u_*}\frac{dU_0}{dx} = -\Pi, \quad \frac{U_0}{u_*^2}\frac{d}{dx}(\Delta u_*) = 1 + 2\Pi, \quad \frac{U_0}{u_*} = \frac{1}{\kappa}\ln\frac{\Delta u_*}{\nu} + A(\Pi).$$

No general solution to the set (5.5.36, 5.5.41, 5.5.43) is known. Approximate solutions, however, can easily be obtained if the very slow change of U_0/u_* with respect to x is exploited. If the range of values of x for which an

approximate solution is desired is fairly small, it may be assumed that u_*/U_0 is equal to its value at the beginning of the interval ($x = x_i$). If we put

$$\frac{u_*}{U_0} = \left(\frac{u_*}{U_0}\right)_i = \beta_i, \tag{5.5.48}$$

we may replace (5.5.41) and (5.5.43) by

$$\frac{\Delta}{U_0}\frac{dU_0}{dx} = -\beta_i \Pi, \tag{5.5.49}$$

$$\frac{1}{U_0}\frac{d}{dx}(\Delta U_0) = (1 + 2\Pi)\,\beta_i. \tag{5.5.50}$$

In this approximation, the logarithmic friction law has to be ignored. The solution of (5.5.49, 5.5.50) was first given by A. A. Townsend (1956); it reads

$$\frac{\Delta}{\Delta_i} = 1 + \tilde{\gamma}_i\left(\frac{x}{x_i} - 1\right), \tag{5.5.51}$$

$$\frac{U_0}{U_{0i}} = \left[1 + \tilde{\gamma}_i\left(\frac{x}{x_i} - 1\right)\right]^{\alpha}, \tag{5.5.52}$$

where

$$\alpha = -\frac{\Pi}{1 + 3\Pi}, \tag{5.5.53}$$

and

$$\tilde{\gamma}_i = (1 + 3\Pi)\,\beta_i x_i/\Delta_i. \tag{5.5.54}$$

The coefficient $\tilde{\gamma}_i$ is of order $u_* x/\Delta U_0$, so that it is similar to the time-scale ratio γ defined in (5.5.18). The length scale L, defined in (5.5.5) has the value $\Delta_i/\beta_i\Pi$ at $x = x_i$, so that γ_i may be written as

$$\tilde{\gamma}_i = \left(\frac{1 + 3\Pi}{\Pi}\right)\frac{x_i}{L_i}. \tag{5.5.55}$$

The time-scale ratio γ, on the other hand, is given by

$$\gamma = \frac{\Delta}{\delta}\,\Pi^{-1}. \tag{5.5.56}$$

The singularity of (5.5.56) in the limit as $\Pi \to 0$ is due to the particular way

in which L is defined. If $\Pi = 0$, (5.5.50) yields $d\Delta/dx = \beta_i$, which corresponds to finite values of $\Delta U_0/xu_*$, so that again the ratio of time scales is finite. It should be noted that Δ/δ is always finite if δ is defined as the value of y where F is some small number (say 0.1).

It is clear that (5.5.51) and (5.5.52) are singular if $\Pi \to \infty$. This singularity has physical significance, because it represents flows that are approaching separation. According to (5.5.52) and (5.5.53), this occurs if $U_0 \propto x^{-1/3}$. In experimental practice, no steady, stable flows at $\Pi > 10$ can be obtained. Equation (5.5.51) also shows that equilibrium layers become thicker more rapidly at large positive values of Π. It should be noticed that all boundary layers grow linearly in x if u_*/U_0 is assumed to be constant. For large values of $(x - x_i)$, the slow decrease of u_*/U_0 with Δ (and thus with x) takes effect; the boundary-layer thickness then increases roughly as $\delta \propto x/\ln x$.

Boundary layers in zero pressure gradient A somewhat more detailed discussion of the case $\Pi = 0$ (corresponding to constant U_0) is in order. If the pressure gradient is zero, (5.5.42), (5.5.43), and (5.5.36) become

$$-\eta \frac{dF}{d\eta} = \frac{dG}{d\eta}, \tag{5.5.57}$$

$$\frac{U_0}{u_*^2} \frac{d}{dx}(\Delta u_*) = 1, \tag{5.5.58}$$

$$\frac{U_0}{u_*} = \frac{1}{\kappa} \ln \frac{\Delta u_*}{\nu} + A(0). \tag{5.5.59}$$

The short-range growth of Δ may be approximated by

$$\frac{d\Delta}{dx} = \beta_i, \tag{5.5.60}$$

where β_i is the value of u_*/U_0 at x_i. In the case $\Pi = 0$, $\Delta/\delta \cong 3.6$ if δ is defined as the value of y where $F = -0.1$.

It is worthwhile to consider the entrainment of fluid outside the boundary layer by the turbulent motion at the edge of the boundary layer. The continuity equation may be integrated to yield

$$V_0 = -\int_0^\infty \frac{\partial U}{\partial x}\, dy = -\frac{d}{dx}\left(u_* \Delta \int_0^\infty F\, d\eta\right). \tag{5.5.61}$$

Since the integral in (5.5.61) is equal to -1 by virtue of (5.5.44), we may

write for the slope α_0 of the mean streamlines at the edge of the boundary layer

$$\alpha_0 \cong \tan\alpha_0 = \frac{V_0}{U_0} = \frac{1}{U_0}\frac{d}{dx}(\Delta u_*) = \frac{d\delta^*}{dx}, \tag{5.5.62}$$

where δ^* is the *displacement thickness* (5.5.66). By substitution of (5.5.58) we find that

$$\alpha_0 = (u_*/U_0)^2. \tag{5.5.63}$$

The average slope α_δ of the edge of the boundary layer is $d\delta/dx \cong 0.28\, d\Delta/dx$ if $\Delta/\delta \cong 3.6$. From (5.5.58) and (5.5.37) we conclude that

$$\alpha_\delta = \frac{d\delta}{dx} \cong \frac{0.28}{U_0/u_* - 1/\kappa}. \tag{5.5.64}$$

If $u_*/U_0 \ll 1$, $\alpha_\delta \gg \alpha_0$. A few numbers may be helpful. If $U_0/u_* = 30$, $\alpha_0 \cong 0.064^\circ$ and $\alpha_\delta \cong 0.57^\circ$. If $U_0/u_* = 20$, $\alpha_0 \cong 0.14^\circ$ and $\alpha_\delta \cong 0.92^\circ$. Figure 5.18 illustrates the situation. The entrainment process is believed to be maintained by large-eddy motions like those sketched in the figure. These

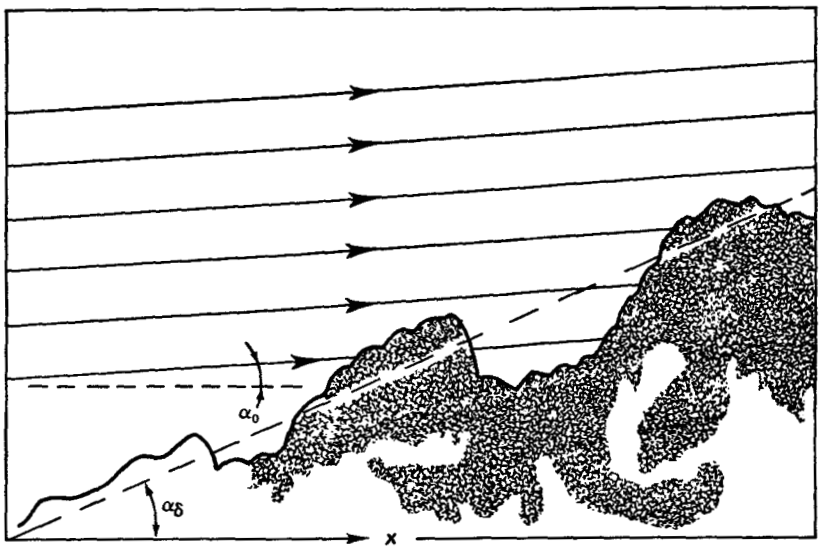

Figure 5.18. Entrainment by a boundary layer in zero pressure gradient. The mean streamlines do not represent the actual flow pattern over the interface shown.

eddies continually distort the interface between the turbulent and nonturbulent fluid and may on occasion engulf parts of the nonturbulent fluid. The entrainment velocity is about $0.28u_*$ if $1/\kappa$ is neglected compared to U_0/u_* and if α_0 is neglected compared to α_δ. The interface between the turbulent boundary layer and the potential flow is quite sharp; its characteristic thickness is believed to be of order ν/u_*, which is comparable to the thickness of the viscous sublayer (Corrsin and Kistler, 1954).

The momentum integral (5.5.58) is associated with the linearized equations of motion. This implies that the momentum thickness θ, defined by

$$U_0^2\theta \equiv \int_0^\infty U(U_0 - U)\, dy, \tag{5.5.65}$$

has been assumed to be equal to the displacement thickness δ^*, defined by

$$U_0\delta^* \equiv \int_0^\infty (U_0 - U)\, dy. \tag{5.5.66}$$

This approximation, of course, is consistent with the assumption that the velocity defect $U_0 - U$ is small compared to U_0. Experiments have shown that the velocity-defect law is satisfied rather accurately even if the velocity defect is not small. Substitution of (5.5.28) into the definitions of δ^* and θ yields for the *shape factor* $H \equiv \delta^*/\theta$

$$H = (1 - C\,u_*/U_0)^{-1}, \tag{5.5.67}$$

where

$$C = \int_0^\infty F^2\, d\eta. \tag{5.5.68}$$

The value of C is about 6 for $\Pi = 0$. If $u_*/U_0 = 0.04$, $H \cong 1.3$, which is 30% larger than the asymptotic value, which is 1. In semiempirical calculations of the downstream development of turbulent boundary layers, H is often assumed to be constant, but u_*/U_0 is allowed to vary according to some empirical friction law (empirical friction laws express the *friction coefficient* c_f, defined as $2u_*^2/U_0^2$, as a function of some power of the Reynolds number $\theta U_0/\nu$).

The distribution of the Reynolds stress, $G(\eta)$, can be computed from (5.5.57) if $F(\eta)$ is known from experiments (see Figure 5.17). For small values of η, F is logarithmic, so that (5.5.57) gives

$$dG/d\eta = -1/\kappa \quad \text{for } \eta \to 0. \tag{5.5.69}$$

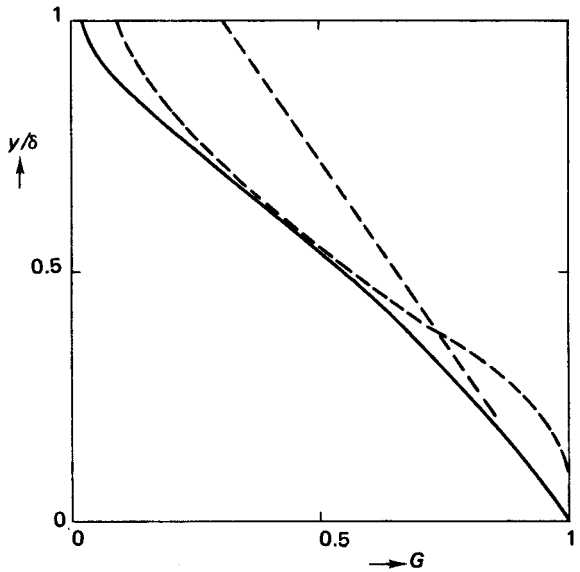

Figure 5.19. The Reynolds-stress distribution for $\Pi = 0$. The solid line is computed with (5.5.57) and F given by Figure 5.17. The straight dashed line is (5.5.70), with $1/\kappa = 2.5$, $\Delta/\delta = 3.6$. The curved dashed line is (5.5.72), with $K = 1/60$.

Since $G \to 1$ if $\eta \to 0$, (5.5.69) may be integrated to yield

$$G(\eta) = 1 - \eta/\kappa. \tag{5.5.70}$$

This expression is valid only near the surface. Figure 5.19 gives a sketch of the distribution of $G(\eta)$.

Equation (5.5.57) relates the velocity profile to the stress profile. So far, we have avoided any assumptions on the relation between stress and velocity gradient. With similarity arguments and asymptotic rules, we have resolved all of the essential features of boundary-layer flows without ever solving the equations of motion. If we want to solve equations like (5.5.57), we need a constitutive relation to link the stress to the velocity gradient. A simple constitutive relation is

$$G = K\, dF/d\eta, \tag{5.5.71}$$

where K is an eddy viscosity, nondimensionalized with u_* and Δ. If K is independent of η, (5.5.57) and (5.5.71) can easily be solved for the stress G. The result is

$$G(\eta) = \exp(-\eta^2/2K). \tag{5.5.72}$$

The value of K, of course, has to be determined by curve fitting. A curve according to (5.5.72), with $K = \frac{1}{60}$, has been drawn in Figure 5.19. The velocity distribution $F(\eta)$ can be obtained from (5.5.72) by integrating once more. This introduces an arbitrary integration constant, which can be adjusted in such a way that the resulting curve is close to the logarithmic velocity profile at small values of η. This is hardly worth the effort, though; if an analytical expression for $F(\eta)$ is desired, a sinusoidal wake function of suitable amplitude does just as well.

Transport of scalar contaminants Within the scope of this book, it is impossible to discuss the transport of heat or other scalar contaminants in turbulent boundary layers in any detail. Let us briefly consider passive contaminants that are released from the surface (for example, the heat flux through a boundary layer on a hot wall). If the ratio of the kinematic viscosity to the diffusivity of the contaminant is near unity, the distribution of the contaminant is similar to the distribution of the mean-velocity defect; the rate of spread of contaminant in the y direction is the same as the rate of growth of the boundary layer. The rate of transfer of contaminant away from the surface is coupled to the stress at the surface. In the case of temperature, the transfer law reads

$$\frac{\Theta_w - \Theta_0}{\theta_*} = \frac{1}{\kappa} \ln \frac{\Delta u_*}{\nu} + \text{const}, \tag{5.5.73}$$

where

$$\theta_* \equiv H/\rho c_p u_*. \tag{5.5.74}$$

In these expressions, it has been assumed that the thermal diffusivity is equal to ν. The rate of heat transfer from the surface, H, can be computed if the temperatures at the surface (Θ_w) and outside the boundary layer (Θ_0), as well as u_* and Δ, are known.

If the diffusivities for the scalar and for momentum are not the same, the thickness of the viscous (momentum) sublayer and of the molecular diffusion layer of the scalar near the surface are not the same. The transfer of scalar contaminants through the boundary layer then becomes a very complicated problem. A case in point is heat transfer in turbulent flow of liquid mercury. In mercury at room temperature, the thermal diffusivity (γ) is 35 times as

large as the kinematic viscosity. If the transport of heat by turbulent motion is represented by an eddy diffusivity γ_e, which is about $u_*\Delta/60$, the ratio γ_e/γ becomes equal to one for $u_*\Delta/\nu \sim 2{,}000$. At moderate Reynolds numbers like this, much of the heat transfer is caused by molecular motion, even though nearly all of the momentum transfer is caused by the turbulent motion. Effectively, the molecular diffusion layer extends through the entire momentum boundary layer.

Problems

5.1 Consider fully developed turbulent flow in a two-dimensional diffuser with plane walls. Estimate the opening angle of the diffuser for which the downstream pressure gradient is equal to zero.

5.2 Describe the radial distribution of the circulation and of the mean tangential velocity in a turbulent line vortex. The circulation outside the turbulent vortex is constant; it has a value Γ_0. This is an inner-outer layer problem. The inner core of the vortex is in solid-body rotation; it has negligible Reynolds stresses. For the equations of motion in cylindrical coordinates, see Batchelor (1967) or other texts.

5.3 Estimate the volume flow in the Gulf Stream. This flow is due to the flow in the Ekman layer of the North Atlantic Ocean. Assume that the Ekman layer is driven by westerly winds across the Atlantic at middle latitudes. The wind speeds are of order 10 m/sec. What is the direction of the volume flux in the Ekman layer?

5.4 Experiments have shown that small amounts of high molecular weight, linear polymers added to water can cause a substantial drag reduction in turbulent pipe and boundary-layer flow of water. No satisfactory explanation of this phenomenon has been found, but an appreciation for the order of magnitude of this effect can be obtained by assuming that the polymer solution doubles the viscosity experienced by the turbulence without changing the viscosity experienced by the mean flow. Obtain an estimate for the drag reduction on basis of this assumption. An analysis of the effects of polymers on Figure 5.5 is helpful.

5.5 Write an equation for the kinetic energy $\frac{1}{2}U^2$ of the mean velocity in fully developed turbulent flow in a plane channel. Sketch the distributions of all terms across the channel. Use the data in Figures 5.6, 5.7, and 5.8 whenever needed to obtain reasonable accuracy. The energy exchange between the core region and the wall layers is of particular interest. Interpret your results carefully.

5.6 Repeat the analysis of Problem 5.5 for a turbulent boundary layer over a plane wall without pressure gradient.

5.7 From the data in Section 5.5, obtain an approximate friction law of the type $c_f = \alpha R_\theta^{-\beta}$ ($c_f = 2(u_*/U_0)^2$, $R_\theta = \theta U_0/\nu$, θ is the momentum thickness) for turbulent boundary layers in zero pressure gradient. Integrate the momentum integral equation ($c_f = 2\,d\theta/dx$ if $dP/dx = 0$) to obtain an approximate drag formula for a plate of length L.